Pervasive decreases in living vegetation carbon turnover time across forest climate zones

SUPPORTING ONLINE MATERIAL

Quantification of living vegetation carbon turnover time

Quantification of living vegetation carbon turnover time requires time series data of carbon stock and NPP. Carbon stock is quantified as a point measurement at a given time (plot census) and can change with time while NPP and carbon loss are variables quantified over the time interval between plot censuses. Thus, in this study the instantaneous living vegetation carbon turnover time is quantified as carbon stock in the previous time step divided by carbon loss in the current time interval. In forest plot data, we considered only long-term forest plots that did not experience disturbances such as fires or harvest during the measurement period. Carbon stock, defined as aboveground carbon in living vegetation with time, was quantified using equation (2). NPP was quantified including components of recruitment of new trees and growth of surviving trees while carbon loss was quantified through tree mortality in each census interval. Carbon stock (kg m^{2-}) was normalized by diving by plot area, while NPP (kg m^{2-} y^{-1}) and carbon loss (kg m^{2-} y^{-1}) were normalized by diving by plot area and time interval. In analysis of remote sensing and Earth system models, estimates or outputs of NPP and vegetation carbon stock were used to quantify carbon turnover time using equations (1-3).

Forest plot data

Forest plot data used in this study was screened according to the following criteria: (1) all plots had at least three consecutive censuses, which allowed for calculations of NPP, carbon loss, changes of vegetation carbon stock, and thus τ over the least of two different time intervals. (2)

Plots were natural, unmanaged forest stands that have not been disturbed by fires, harvesting, floods, avalanches, or other manmade damage. A few plots affected by leaf miners or bark beetles, in particular in Alaska, were also included in our studies because leaf miners or bark beetles usually interact with drought (one major driver tested here) to accelerate tree mortality and carbon turnover time and inclusion of these plots made coverages of forest plots more comparable to estimates of remote sensing and Earth system models. (3) As a general rule, plots had records of individual trees with a certain size and its status (i.e., dead, live, or recruited) and these individuals were clearly marked and repeatedly measured. (4) Diameter of every tree above a defined diameter at breast height (DBH = 1.3 or 1.4 meter) (but with exceptions for non-cylindrical stems owing to buttresses or other deformities) was recorded in each census, thus allowing for quantifications of vegetation biomass using allometric equations. (5) All plots had long-term (>9 years) observations between the first and last census allowing for the evaluation of decadal-scale changes in carbon turnover time and the relationship with potential drivers. (6) All plots had positive values of growth. (7) The plots were categorized as mature or old-growth forests to avoid the substantial impacts associated purely with successional dynamics. (8) Plots had at least two finite values of carbon turnover time over consecutive censuses.

We acquired the data meeting these criteria through an extensive literature review and an assessment of long-term forest monitoring sites. The complied data meeting these criteria included plots in tropical tropical (n = 128), temperate (n = 87) and cold climate zones (n = 480) ranging in time period from 1955 to 2018 in South America, North America, and Europe. The Köppen-Geiger climate classification was used to determine the climate zones (i.e., tropical, temperate and cold) of these forest plots. Supplementary Table S1 summarized the number of plots, total area, earliest/latest data of census, total number of census, and data source or providers in each forest climate zone. Supplementary excel file S1 lists other information in details including plot code, latitude, longitude and elevation (if available), climate zone, plot size, start/end census data, number of census for each plot.

The majority of forest data in tropical climate zone were from the published study by Brienen et al (2015) (1), who compiled data of total 321 plots spanning every tropical South American country except Suriname. Of the 321 plots, 101 plots located in Bolivia, Brazil, Colombia, Ecuador, French Guiana, Guyana, Peru, and Venezuela from RAINFOR plot network met the criteria of our study. Here, we provided a summary for these plots. Data usage for our study and quantification of variables such as carbon stock, NPP, and carbon loss (tree mortality) in our study and more information can be referred to in details in Brienen et al (2015). The forest plots compiled by Brienen et al (2015) were mature forests across the lowland tropical areas of South America. Aboveground biomass was quantified using allometric equations, which had terms for woody density, diameter and tree height (2). The global wood density database was used to determine the wood density values (3). The established diameter-height relations were used to estimate values of height. Tree diameter was usually measured at breast height (1.3 m) following standard protocol. For the trees with non-cylindrical stems owing to buttresses or other deformities, the height of diameter measurement was raised approximately 50 cm above deformities or was changed to a new plant height between consecutive censuses. The methods in Talbot et al (2010) and Clark et al (2013) (4, 5) were used to account for the changes of plant height in diameter measurement and then derive more reliable records of diameter. Moreover, several techniques in Talbot et al (2010) were used to account for missing diameter values, typographical errors, and extreme diameter growth so that the potential errors were avoided or minimized. Specific to tropical forests, following the method in Talbot et al (2010), the effects of varying census interval length were accounted for by estimating unobserved recruits and unobserved biomass growth and mortality (6, 7). For the purpose of our study, we used the available data as published in Brienen et al (2015). We used aboveground biomass (AGB) at the start of the census (kg m^{-2}), annual net change in AGB (kg m^{-2} y^{-1}), and interval time (y) between consecutive censuses to derive the AGB in each census. Total annual AGB mortality (plus added unobserved components) (Mg ha^{-1} y^{-1}), total annual AGB productivity of surviving trees plus recruitment (plus added unobserved components) (Mg ha^{-1} y^{-1}), and interval time between consecutive censuses were used to determine NPP (Mg ha^{-1} int^{-1}) and mortality (Mg ha^{-1} int^{-1}) in each census interval, respectively.

Additional data for forests in tropical climate zone were provided by the Smithsonian Tropical Research Institute (9 plots, hereafter called STRI plots) and CARBONO project conducted in La Selva biological station (18 plots, hereafter called CARBONO plots). The STRI plots included 50-hectare plot at Barro Colorado Island, Panama with 8 censuses from 1982 to 2015 and the other 10 plots with 3 censuses in Panama. AGB was quantified by allometric equations (8). Further details are available at http://ctfs.si.edu/Public/CTFSRPackage/index.php/web/topics/biomass~slash~biomass.CTFSdb.r/biomass.CTFSdb. The CARBONO plots were from a network of 18 0.5-ha permanent and old-growth forest plot plots across gradients of slope ($<3^{\circ}$ to ~21°) and soil nutrients (2-3-fold for most nutrients, e.g., phosphorus, potassium) at the La Selva Biological Station, Costa Rica. These plots were censused annually from 1998 to 2014. In CARBONO plots, two methods were used to determine AGB; the method based on only diameter and the method also incorporating wood density gave slightly (8%) different estimate of AGB (5). This study used the available data of ABG based on the simpler Brown allometry (only diameter) (9). For both STRI and CARBONO plots, NPP was determined as AGB productivity of surviving trees plus recruitment or new trees and mortality was determined as AGB loss when trees were recorded dead in each census interval.

A portion of data for forests in temperate climate zone comprises plots from van Mantgem (10). van Mantgem et al (2009) compiled data of 76 plots which were more than 200 years old across Pacific Northwest, California, and interior in the United States. We note that all of these 76 plots were classified as forests in temperate climate zone, consistent with Mantgem et al (2009), while few plots were forests in cold climate zone according to the Köppen-Geiger climate classification. These data were compiled by examining an extensive literature review and contacting colleagues at long-term forest research sites such as those in the USDA Forest Service's Experimental Forest and Research Natural Area networks. Only plots which were ≥ 0.25 ha and contained >100 trees at the first census were included. Diameter of every tree above a defined diameter at breast height (1.4 meter) was repeatedly measured across censuses. In total, we used the available data (tree diameter and tree status: recruitment or death) of 63 plots which met our requirement.

A portion of data in forest in cold climate zone were acquired from the Cooperative Alaska Forest Inventory and from the Canadian Forest Inventory (11, 12). Here we summarized the information about these plots and more information can be referred to in details in Malone et al (2009) and Peng et al (2011). The Cooperative Alaska Forest Inventory (CAFI) permanent sample plots were established in 1994. All of the forest plots were square and 0.04 ha. In our study, only trees with diameter at breast height > 3.8 cm were included to avoid bias resulting from a change in the definition of minimum tree size during the study interval. The CAFI recorded insect damage and classified the damage as “minor”, “moderate”, “severe”, and “unspecified”. In this region, plots with potential effects of insect damage were included to increase coverage and representation of forest climate zones comparable to remote sensing data and Earth system models. The original data included young forests and we used the criteria of forest gymnosperm fraction (>40%) to select mature forests (13). In total, 177 plots which meet our requirement were used from CAFI. Peng et al (2011) compiled a total of 96 mature forest stands (≥ 80 years) by extensively reviewing data from permanent sample plots in Alberta, Saskatchewan, Manitoba, Ontario, and Quebec in Canada. Out of the 96 plots, we used the available data (tree diameter and tree status, recruitment or death) from 91 plots to quantify living vegetation carbon turnover time and all plots had a large enough number of live trees (≥ 80) at the first census.

Additional forest data in temperate and cold climate zones were from the Forest Inventory and Analysis (FIA) Program of the U.S. Forest Service and partly from the International Co-operative Programme on Assessment and Monitoring of Air Pollution Effects on Forests (ICP Forests) launched in 1985 under the UNECE Convention on Long-range Transboundary Air Pollution (CLRTAP). The FIA program applies a nationally standardized sampling protocol with a sampling intensity of one plot per 2,428 ha (14). FIA inventory plots in forested areas consist of four 7.2 m fixed-radius subplots spaced 36.6 m apart in a triangular arrangement with one subplot in the center. All trees (standing live and dead), with a diameter at breast height (DBH) of at least 12.7 cm, are inventoried in each subplot. We note that the criteria of 12.7 cm is much higher than those in other temperate and cold forests and thus may underestimate the growth because of limited records of recruitments. For each plot, the age is determined by coring three dominant or co-dominant trees that represent a plurality of non-overtopped trees. The stand age is estimated as the average of these three trees (14), assuming that the age of the dominant or codominant trees represents the age of the forest ecosystem. The FIA data were extracted from 1998 – 2018 with three censuses and we excluded plots that reported any human-caused disturbances, such as fire, logging and were less than 120 years old for forest in temperate climate zone and 100 years old for forest in cold climate zone (14). Of the FIA forest data, 196 forest plots in cold climate zone and 12 forest plots in temperate climate zone defined by Köppen-Geiger climate classification were used, respectively. For the ICP Forests data, we excluded the plots that were thinned, cut or strongly affected by windthrows. Following the previous study (15), we used the criteria of tree density (n > 1000 per ha) and median value (<24 cm) of dbh to exclude young forests. In total, 12 plots in temperate climate zone and 16 plots in cold climate zone located in Europe met the criteria of our study. The standard protocol for vegetation survey and tree measurements is described in Dobbertin and Neumann (2016) (16).

In tropical forest plots and FIA forest plots, we used available biomass data. In other forest plots in temperate and cold climate zones, we used allometric equations relating biomass to DBH to quantify vegetation biomass. We used the published studies to determine the suitable allometric equations specific to the species. When there was more than one equation for the same species, we determined the equations using three standards: (1) the range of DBH of species in plots in our study was within the range of DBH of species of allometric equations; (2) allometric equations had the highest coefficient of determination; (3) allometric equations estimated different biomass components (i.e., aboveground biomass, stems, or bark) and we were interested in vegetation biomass. When the allometric equations were not available (i.e., species *Pinus flexilis* and *Taxus brevifolia*) we used the values of coefficients of allometric equations in the same genus species with similar locations. The allometric equations for species in North

America (USA and Canada) were based on Jenkins et al (2004) (17), while the allometric equations for species in Europe were mainly based on Forrester et al (2017) (18) who synthesized the biomass allometric equations for European tree species. For some species (<20%) in which the biomass allometric equations are not available, we conducted an extensive reviewing of other published studies to determine the biomass allometric equations (18–28). Supplementary excel S2 listed the information of species, equations, and biomass component used in this study. In all forest plot data analysis, vegetation biomass was converted to carbon stock assuming that 50% of biomass is carbon (8). NPP, carbon loss, carbon stock, and living vegetation carbon turnover time were quantified in each forest plot using equations (1), (2), and (3).

Remote sensing data

NPP and carbon stock data required to quantify temporal changes in carbon loss and carbon turnover time were derived from satellite remote sensing. Annual carbon stock data (0.25 × 0.25°) ranged from 1993 to 2012 and were derived from the published study in Liu et al (2015) (29). Liu et al (2015) estimated carbon stocks based on harmonized vegetation optical depth (VOD) derived from a series of passive microwave satellite sensors, based on the proportionality of VOD and total vegetation water content of vegetation, which is closely related to total aboveground biomass. Estimates of carbon stocks were derived from VOD timeseries based on statistical relationships between VOD and high-resolution estimates of pan-tropical aboveground biomass and the simplifying assumption that aboveground biomass is 50% carbon. Since VOD is sensitive to inland water bodies, pixels influenced by these features were filled using nearby grid cells with the same landscape type. The annual NPP data (0.25 × 0.25°) used in this study ranged from 1993 to 2011 and were derived from the published study in Smith et al. (2015) (30). The NPP quantification is based on the Moderate Resolution Imaging Spectroradiometer (MODIS) NPP algorithm, driven by the fraction of photosynthetically active radiation (FPAR) absorbed by the vegetation and leaf are index (LAI) data. Two versions of NPP data, one in which climate data were used in the calculation and one in which climate data were fixed to isolate the influence of satellite observations alone, were available. Sensitivity testing showed that these two data sets gave very similar results of temporal trends in NPP, carbon stock, mortality and carbon turnover time across forest climate zones.

While the NPP and carbon stock are satellite observation-based datasets, it should be cautioned that they also rely on algorithm assumptions and parameters, and these factors introduce significant potential uncertainty in long-term trends. For instance, satellite-derived FPAR and LAI products have been found to exhibit large discrepancies, especially across tropical forest regions, and thus drive significant uncertainty across satellite-derived NPP estimates (31). Satellite-derived NPP data used here may underestimate the effect of CO_2 fertilization, which thus may underestimate long-term positive trends of NPP (32). Satellite-derived NPP and to a lesser extent carbon stock estimates are prone to saturation, especially in areas of dense evergreen forests (33, 34). Satellite-derived C stock estimates may be biased and mostly capturing canopy dynamics, especially since these estimates were derived from X-band VOD data, which are known to penetrate only the vegetation surface in dense forests (35). Additionally, the temporal extent of the satellite data analyzed was limited to the time range 1993 to 2011 due to data availability, which is a relatively short period of time to detect statistically meaningful trends. Despite these considerable limitations, we find general consistency between forest inventory-based and satellite-based estimates of living vegetation carbon turnover times across climate zones except temperate climate zone, which provides additional independent support for a robust large-scale signal. New satellite platforms, including NASA Orbiting Carbon Observatory 3 (OCO-3) and Global Ecosystem Dynamics Investigation (GEDI), could greatly improve our ability to track NPP and aboveground C stocks from space, respectively. This would greatly improve our ability to monitor changes in aboveground vegetation turnover in future (36).

Advanced Very High Resolution Radiometer (AVHRR) Continuous Fields Tree Cover Product (1 kilometer) was used to define the forest climate zones (37) using the standard of tree cover more than 30% (38), while sensitivity tests suggest the results reported in the main text are robust to the scenarios of 20% and 25%. The world map (0.5 × 0.5 degree) of the Köppen-Geiger climate classification was used to determine the climate zones (i.e., tropical, temperate and cold), following the criteria: tropical (BSk; Csa; Csb); temperate (Csa, Csb, Csc, Cwa, Cwb, Cwc, Cfa, Cfb, Cfc); Cold (Dsa, Dsb, Dsc, Dsd, Dwa, Dwb, Dwc, Dwd, Dfa, Dfb, Dfc, Dfd) (39). The Global Human Footprint Dataset (hereafter called HFI) (1 kilometer) of the Last of the Wild Project, Version 2, 2005 (LWP-2) expressed as a percentage was used to account for the potential influence of human activities (http://sedac.ciesin.columbia.edu/data/set/wildareas-v2-human-footprint-geographic). Data of GFED4 biomass burning emissions (0.25 × 0.25°) expressed as percent annual burn area (PABA) were used to account for the potential impacts of fires. PABA ranged from 1996 to 2015 and thus we used average values over the time period in this study. Because our study investigates the impacts of CO_2 and climate change, we excluded the places where values of HFI or PABA were high and thus influence of humans or fires would be significant. To this end, we examined a variety of HFI and PABA values and determined to use the value of HFI < 30% and PABA < 10% (called baseline) to define forest climate zones without or with minimal influence of humans and fires. This standard gave a good representation of forest climate zones and is also relatively comparable to our forest plot data. The Supplementary table S2 listed the ratio (%) of total number of pixels in other HFI and PABA values to the case in baseline. The results showed that this ratio was not sensitive to values of PABA across forest climate zones but showed a moderate sensitivity to values of HFI especially in temperate forests. Integrating all of the data resampled to the spatial resolution of $0.25 \times 0.25°$ (when necessary), we classified the global forest climate zones into tropical, temperate, and cold without or with minimal influence of human activities and fires. The classified spatial extent across forest climate zones was consistent between remote sensing data analysis and earth system models (see the section of earth system models for details).

Earth system models

To quantify carbon loss and living vegetation carbon turnover time, we analyzed the simulated outputs of vegetation carbon stock (C_{veg}) and NPP from eight Earth system models in phase 5 of the Coupled Model Intercomparison Project (CMIP5) (CanESM2, CCSM4, GFDL-ESM2G, HadGEM2-ES, IPSL-CM5A-MR, MIROC-ESM, MPI-ESM-LR, NorESM1-M). In our forest plots, NPP was quantified as increment of aboveground vegetation carbon including components of recruitment of new trees and growth of surviving trees. By comparison, in Earth system models NPP is the increment of total vegetation carbon which also included belowground components. We used C_{veg} and NPP in Earth system models because data of NPP allocating to leaves and wood were only available in one of these eight Earth system models (i.e., IPSL-CM5A-MR). However, we conducted a sensitivity test by using the estimates of aboveground vegetation carbon stock and NPP derived from IPSL-CM5A-MR including the components of leaves and wood and the results showed no appreciable difference. The ensemble member used to account for variations in initial states, initialization methods or physics details was r1i1p1. To correspond to the earliest date (1955) of forest plot data, we extracted data from the historical all-forcing scenario simulations from 1955 to 2005. The future climate scenario simulations were from 2006 to 2100 and model outputs used were carried out in the scenario of Representative Concentration Pathways (RCP) 8.5 to bracket the full range of potential climate change. The original model outputs (monthly C_{veg} and NPP) were converted to values on annual time scale to quantify NPP, C_{veg}, carbon loss and carbon turnover time using equations (1-3). The eight Earth system models have different spatial resolution. To make the results more comparable, the outputs of eight earth system models were resampled at a spatial resolution of 0.25 × 0.25° using the bilinear method, comparable to the resolution of our remote sensing data.

CO_2 and climate data

We used historical and projected annual CO_2 concentrations (RCP 8.5) assuming no spatial variation downloaded from https://tntcat.iiasa.ac.at/RcpDb/dsd?Action=htmlpage&page=download. For our forest plot analysis, climate data of annual precipitation and temperate used for temperate and cold forests were acquired from Climate data for North America (ClimateNA) (https://sites.ualberta.ca/~ahamann/data/climatena.html) with a spatial resolution of 1 km. For our forest plots located in the tropical climate zone, as well as temperate and cold climate zones in Europe, ClimateNA was unavailable. Thus we used the Climatic Research Unit (CRU) Time-Series (TS) version 4.00 of high-resolution (0.5 × 0.5 km) gridded annual climate data. Latitude, longitude and elevation (if available) of each plot were used to extract climate data based on proximity of forest plots. To evaluate the dependence of temporal trends of forest growth, carbon loss and living vegetation carbon turnover time on climate, mean values of annual climate (precipitation and temperature) and its anomaly were quantified for each census interval. Climate anomalies were quantified as Z-scores. The climate data used in Earth system models were derived from their own model outputs on the monthly time scale. All climate data were converted to values on the annual time scale.

Statistical analyses

Two approaches were used to quantify temporal trends of NPP, carbon stock, carbon loss, and living vegetation carbon turnover time in remote sensing and Earth system models. First, consistent with forest plot data, NPP, carbon stock, carbon loss, and living vegetation carbon turnover time were natural log-transformed before analysis. Second, the dependent "variable" was percent change (%/year) and quantified as an increase or reduction relative to initial value of each dependent variable. In both approaches, to meet the requirement of normal distribution of residual in linear mixed models, values of each dependent variable more than 97th percentile and less than 3th percentile (baseline; ≈6%) were removed as outliers prior to analysis of linear mixed models. The results of the two approaches showed very similar patterns in Earth system models, while the patterns were not completely consistent in some climate zones in remote sensing analysis. To make the results directly comparable between forest plot and Earth system models, we thus used the first approach to present the results of temporal changes in each dependent variable at scales of climate zones (Fig. 3A; *SI Appendix*, Fig. S6). By comparison, at global scale of every pixel we chose the second approach to better visualize the temporal changes in each dependent variable and the spatial variations in temporal changes in each dependent variable (see *SI Appendix* for details) (Fig. 3C; *SI Appendix*, Fig. S12).

The analysis of using linear mixed models to account for each plot or pixel as a random effect was compared with the method by Friend et al (2014). Friend et al (2014) method used in this study aggregated the values of NPP, carbon stock, carbon loss, and then quantified living vegetation carbon turnover time in each forest climate zone. The area of pixels depended on locations. Thus, during the aggregation of values to each forest climate zone, we accounted for the difference of area in each pixel in different forest locations. Linear regression models were then used to quantify their temporal trends at scales of forest climate zones. The results showed that in the remote sensing analysis, these trends (analyzed using linear mixed-effects models to account for random effects in each pixel) differed from the method of regionally aggregating NPP and vegetation carbon stock to quantify trends in living vegetation carbon turnover time by simple linear regression (40), which indicated dampened and none significant changes in forest climate zones (*SI Appendix*, Fig. S4). Patterns detected by aggregating variables on large (biome to global) scales may misrepresent processes on local scales (41), e.g. by averaging over high spatial heterogeneity in trends of carbon turnover time (*SI Appendix*, Fig. S11).

To test the robustness of the results using equation (4), some potential important factors that affected changes in demographic rates due to basal area (competition) and succession and spatial autocorrelations were accounted for by including these factors into equation (4) (42). The potential important factors accounted for were standardized basal areas (Bas) and competition index (SDI) in temperate and cold climate zones, while such data are not available in tropical forest plot data and analysis of remote sensing and Earth system models. Competition index was quantified following the method by Zhang et al (2015) (42), which included terms of number of trees per hectare and the quadratic mean DBH. The Moran's I test showed no significant influences of spatial autocorrelations except for NPP and carbon stock in cold forests in the residuals of linear mixed models used in this study (Table S3; Table S4).

To examine the effects of climate anomaly, we also included rainfall and temperature variability (VPrn and VTAS) into Eqn (5). In Earth system models, the annual time series of climate data precluded our capability of quantifying the impacts of climate anomaly. Independent variables in equations (5) were standardized (z-score) before analysis. Analysis by a matrix of pairwise correlations and variance inflation factors showed that climate data had high collinearity in future climate scenarios in Earth system models. Thus equation (5) was analyzed in historical climate scenario.

To evaluate the averaged predictions of vegetation carbon turnover time, ensemble mean of carbon turnover time in Earth system models was quantified in two ways: (1) carbon turnover time in each Earth systems model grid cell was quantified and then all grid cells were averaged to get ensemble mean of carbon turnover time for analysis of temporal trends; (2) ensemble mean of vegetation carbon stock and NPP were calculated by averaging from eight Earth system models and then ensemble mean of carbon turnover time was quantified for analysis of temporal trends. We found no difference between these two methods, and thus the main text shows the results using method (1).

Given the substantial length of dataset time-series (i.e., historical 1971-2005 and predictive 2006-2100 in CMIP5 models; historical 1993-2011 in remote sensing), we also used simple linear regression to evaluate the global patterns of time trend in percent change of NPP, carbon stock, carbon loss, or living vegetation carbon turnover time at local scales (i.e. each $0.25 \times 0.25°$ grid cell). This allows us to quantify the spatial patterns of temporal changes in growth, carbon loss, and living vegetation carbon turnover time. Forest plot data have limited repeated census at each plot scale and thus do not allow simple linear regression. In our forest plots, the census period of the majority of plots (> 95%) ranged from 1971 to 2018 and thus as a sensitivity analysis we calculated the "historical period" in Earth system models defined to be 1971-2018. In this sensitivity analysis, we merged the historical (1971-2005) Earth system model output with that of Representative Concentration Pathways (RCP) 8.5 for 2006-2018. We note that all of the RCP scenarios show quite similar climate up through the 2020s and thus this is a reasonable approach.

References

1. Brienen RJW, et al. (2015) Long-term decline of the Amazon carbon sink. *Nature* 519:344–348.
2. Feldpausch TR, et al. (2012) Tree height integrated into pantropical forest biomass estimates. *Biogeosciences* 9:3381–3403.
3. Chave J, et al. (2009) Towards a worldwide wood economics spectrum. *Ecol Lett* 12:351–366.
4. Talbot J, et al. (2014) Methods to estimate aboveground wood productivity from long-term forest inventory plots. *For Ecol Manage* 320:30–38.
5. Clark DA, Clark DB, Oberbauer SF (2013) Field-quantified responses of tropical rainforest aboveground productivity to increasing CO2 and climatic stress, 1997-2009. *J Geophys Res Biogeosciences* 118:783–794.
6. Malhi Y, Phillips OL (2004) Tropical forests and global atmospheric change: a synthesis. *Philos Trans R Soc Lond B Biol Sci* 359:549–55.
7. Lewis SL, et al. (2004) Concerted changes in tropical forest structure and dynamics: evidence from 50 South American long-term plots. *Philos Trans R Soc Lond B Biol Sci* 359:421–36.
8. Chave J, et al. (2005) Tree allometry and improved estimation of carbon stocks and balance in tropical forests. *Oecologia* 145:87–99.
9. Clark DB, Clark DA, Oberbauer SF, Kellner JR (2017) Multidecadal stability in tropical rain forest structure and dynamics across an old-growth landscape. *PLoS One* 12. doi:10.1371/journal.pone.0183819.
10. Van Mantgem PJ, et al. (2009) Widespread increase of tree mortality rates in the Western

United States. *Science* 323:521–524.

11. Malone T, Liang J, Packee EC, Pacific Northwest Research Station (Portland Or.) (2009) Cooperative Alaska forest inventory. *Gen Tech Rep PNW* (GTR-785):42 p.

12. Peng C, et al. (2011) A drought-induced pervasive increase in tree mortality across Canada's boreal forests. *Nat Clim Chang* 1:467–471.

13. Trugman AT, Medvigy D, Anderegg WRL, Pacala SW (2017) Differential declines in Alaskan boreal forest vitality related to climate and competition. *Glob Chang Biol*. doi:10.1111/gcb.13952.

14. Zhu K, Zhang J, Niu S, Chu C, Luo Y (2018) Limits to growth of forest biomass carbon sink under climate change. *Nat Commun*.

15. Lehtonen A, Mäkipää R, Heikkinen J, Sievänen R, Liski J (2004) Biomass expansion factors (BEFs) for Scots pine, Norway spruce and birch according to stand age for boreal forests. *For Ecol Manage* 188:211–224.

16. Fischer R, Lortenz M (2011) Forest Condition in Europe, 2011 Technical Report of ICP Forests and FutMon. *Forestry*:212.

17. Jenkins JC, Chojnacky DC, Heath LS, Birdsey RA (2004) *Comprehensive Database of Diameter-based Biomass Regressions for North American Tree Species. General Technical Report NE-319. Newtown Square, PA: Forest Service, Northeastern Research Station*.

18. Forrester DI, et al. (2017) Generalized biomass and leaf area allometric equations for European tree species incorporating stand structure, tree age and climate. *For Ecol Manage* 396:160–175.

19. Aboal JR, Arévalo JR, Fernández Á (2005) Allometric relationships of different tree

species and stand above ground biomass in the Gomera laurel forest (Canary Islands). *Flora* 200:264–274.

20. Ounban W, Puangchit L, Diloksumpun S (2016) Development of general biomass allometric equations for Tectona grandis Linn.f. and Eucalyptus camaldulensis Dehnh. plantations in Thailand. *Agric Nat Resour* 50:48–53.

21. Alberti G, et al. (2005) Aboveground biomass relationships for mixed ash (Fraxinus excelsior L. and Ulmus glabra Hudson) stands in Eastern Prealps of Friuli Venezia Giulia (Italy). *Ann For Sci* 62:831–836.

22. Zianis D, Seura S (2005) *Biomass and stem volume equations for tree species in Europe* doi:citeulike-article-id:11858948.

23. Koukoulomatis KD, Mitsopoulos ID (2007) Crown fuel weight estimation of Black pine (Pinus nigra) plantations in Southern Bulgaria. *Silva Balc* :57–65.

24. Cienciala E, Apltauer J, Exnerová Z, Tatarinov F (2008) Biomass functions applicable to oak trees grown in Central-European forestry. *J For Sci* 54:109–120.

25. Moore JR (2010) Allometric equations to predict the total above-ground biomass of radiata pine trees. *Ann For Sci* 67:806–806.

26. Zianis D, Mencucini M (2010) Aboveground biomass relationships for beech (Fagus moesiaca Cz.) trees in Vermio Mountain, Northern Greece, and generalised equations for Fagus sp. *Silvae Genet* 59:175–182.

27. Worku E (2015) Allometric Equation for Biomass Determination in Juniperus procera Endl. and Podocarpus falcatus Mirb of Wof-Washa Forest: Implication for Climate Change Mitigation. *Am J Life Sci* 3:190.

28. Morhart C, Sheppard J, Schuler J, Spiecker H (2016) Above-ground woody biomass

allocation and within tree carbon and nutrient distribution of wild cherry (Prunus avium L.) – a case study. *For Ecosyst* 3:4.

29. Liu YY, et al. (2015) Recent reversal in loss of global terrestrial biomass. *Nat Clim Chang* 5:470–474.

30. Kolby Smith W, et al. (2015) Large divergence of satellite and Earth system model estimates of global terrestrial CO2 fertilization. *Nat Clim Chang* 6:306–310.

31. Liu Y, et al. (2018) Satellite-derived LAI products exhibit large discrepancies and can lead to substantial uncertainty in simulated carbon and water fluxes. *Remote Sens Environ* 206:174–188.

32. De Kauwe MG, Keenan TF, Medlyn BE, Prentice IC, Terrer C (2016) Satellite based estimates underestimate the effect of CO2 fertilization on net primary productivity. *Nat Clim Chang* 6:892–893.

33. Hilker T, et al. (2014) Vegetation dynamics and rainfall sensitivity of the Amazon. *Proc Natl Acad Sci* 111:16041–16046.

34. Zhou L, et al. (2014) Widespread decline of Congo rainforest greenness in the past decade. *Nature* 508:86–90.

35. Brandt M, et al. (2018) Satellite passive microwaves reveal recent climate-induced carbon losses in African drylands. *Nat Ecol Evol* 2:827–835.

36. Stavros EN, et al. (2017) ISS observations offer insights into plant function. *Nat Ecol Evol* 1. doi:10.1038/s41559-017-0194.

37. DeFries R, Hansen M, Townshend JRG, Janetos AC, Loveland TR (2000) 1 Kilometer Tree Cover Continuous Fields, 1.0. *Dep Geogr Univ Maryland, Coll Park Maryl*.

38. Davis KF, Yu K, Rulli MC, Pichdara L, D’Odorico P (2015) Accelerated deforestation

driven by large-scale land acquisitions in Cambodia. *Nat Geosci* 8:772–775.

39. Peel MC, Finlayson BL, McMahon TA (2007) Updated world map of the Köppen-Geiger climate classification. *Hydrol Earth Syst Sci* 11:1633–1644.

40. Friend AD, et al. (2014) Carbon residence time dominates uncertainty in terrestrial vegetation responses to future climate and atmospheric CO2. *Proc Natl Acad Sci U S A* 111:3280–5.

41. Jung M, et al. (2017) Compensatory water effects link yearly global land CO 2 sink changes to temperature. *Nature* 541:516–520.

42. Zhang J, Huang S, He F (2015) Half-century evidence from western Canada shows forest dynamics are primarily driven by competition followed by climate. *Proc Natl Acad Sci* 112:4009–4014.

Appendix Tables and Figures

Table S1. Summary of the long-term forest monitoring plot data ranging from 1955 to 2018 over at least three censuses across tropical (n = 128), temperate (n = 87) and cold climate zones (n = 480) in South and North America and Europe.

Climate zones	Number of plots	Total area (Ha)	Earliest census (y)	Latest census (y)	TNC	Data source and/or provider
Tropical	128	230	1975	2016	1059	Brienen et al (2015); Clark et al (2017); Richard Condit and Steve Hubbell
Temperate	87	88.5	1955	2018	407	van Mantgem et al (2009); Zhu et al (2018); Josep Peñuelas; Jordi Sardans; Dobbertin and Neumann (2016)
Cold	480	33.6	1963	2018	1591	Malone et al (2009); Peng et al (2011); Zhu et al (2018); Josep Peñuelas; Jordi Sardans; Dobbertin and Neumann (2016)

Note: TNC refers to total number of census; for the plot information in details including plot code, region, latitude, longitude and elevation (if available), climate zone, plot size, start/end census data, number of census, please refer to Supplementary excel S1.

Table S2. The ratio (%) of total number of pixels in other human footprint index (HFI) and PABA (percent annual burn area) values to the case in baseline (HFI = 30 and PABA = 10).

Scenarios	Tropical (%)	Temperate (%)	Cold (%)
HFI = 30; PABA = 10	100	100	100
HFI = 40; PABA = 10	108.4	137.4	109.8
HFI = 20; PABA = 10	76.2	43.0	82.8
HFI = 30; PABA = 5	93.6	93.5	99.2
HFI = 30; PABA = 20	106.2	110.9	100.1

Table S3 P values of Moran's I test for the residual in linear mixed models which quantified the temporal trends of growth (mainly aboveground wood production), carbon stock, carbon loss, and living vegetation carbon turnover time across climate zones.

Variables	Tropical	Temperate	Cold
Carbon turnover	0.36130901	0.93815305	0.99992908
Carbon stock	0.99950123	0.99306134	<0.001
Growth	0.99265755	0.9999805	0.00297992
Carbon loss	0.31423193	0.96936037	0.73369188

Table S4 P values of Moran's I test for the residual in linear mixed models which quantified the correlations between climate variables (CO_2, precipitation and temperature) and temporal trends of growth (mainly aboveground wood production), carbon stock, carbon loss, and living vegetation carbon turnover time across climate zones.

Variables	Tropical	Temperate	Cold
Carbon turnover	0.3579274	0.90492126	0.99992908
Carbon stock	0.99965969	0.99696486	<0.001
Growth	0.99425951	0.99998781	0.00263531
Carbon loss	0.29094568	0.95928981	0.63093186

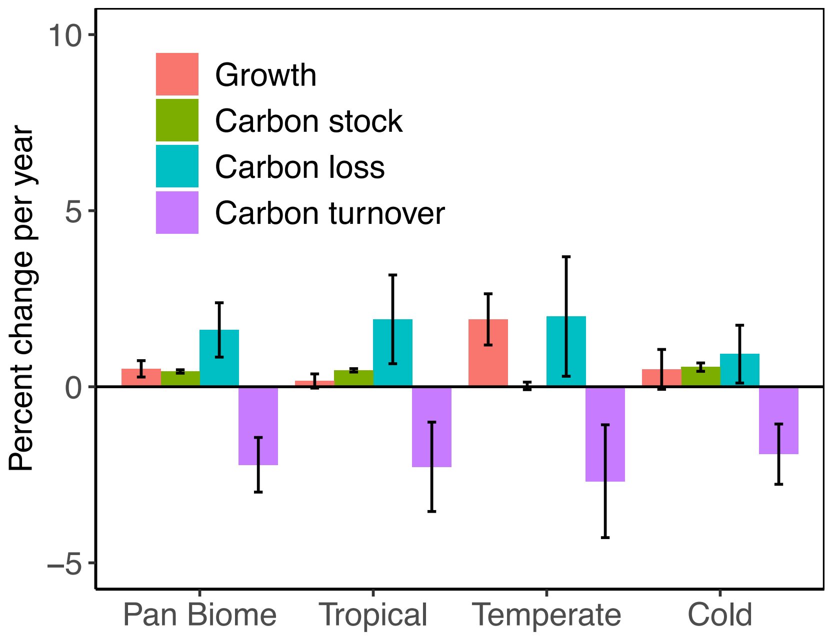

Fig. S1. Percent change per year of growth (kg m^{2-} y^{-1}), carbon stock (kg m^{2-}), carbon loss (kg m^{2-} y^{-1}), and aboveground living vegetation carbon turnover time (y) quantified by forest plot data ranging from 1955 to 2018 over at least three censuses across tropical (n = 128), temperate (n = 87) and cold (n = 480) climate zones. Data were natural log-transformed before analysis. Temporal trends were quantified by linear mixed-effect models accounting for each plot in each forest climate zone as a random effect. The y-axes are coefficient of the independent variable (time) ± 95% CIs. Percent change per year in each variable was quantified as: (exp (β) – 1) * 100, where β is coefficient estimate shown in Figure 2.

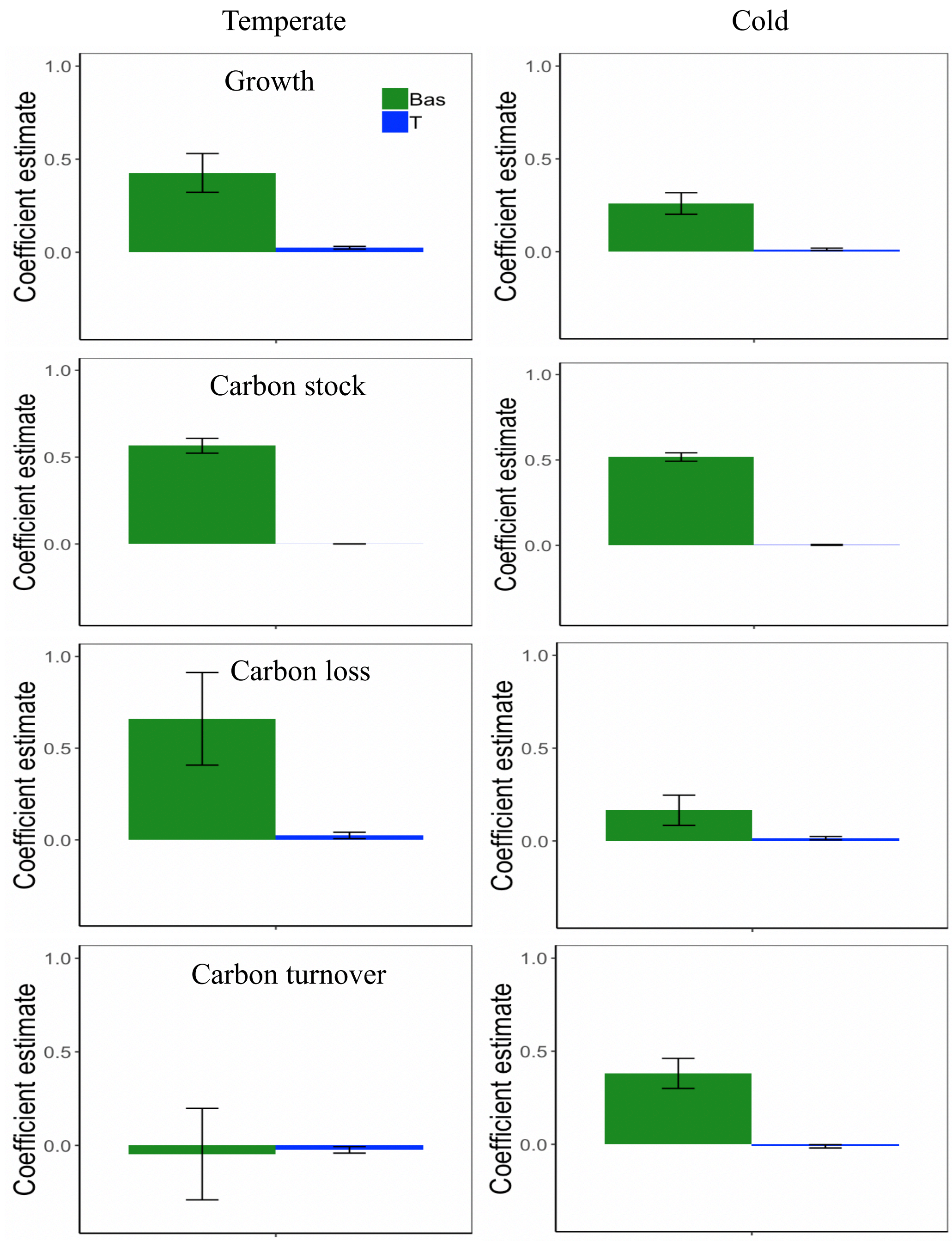

Fig. S2(**A, B**) The relationship between basal area (Bas) and time (T) and growth (mainly aboveground wood production), carbon stock, carbon loss and living vegetation carbon turnover time quantified by forest plot data and linear mixed-effects models in temperate (**A**) and cold (**B**) climate zones. Data of Bas were standardized (z-score) before analysis. Value of y axis is the coefficient of each independent variable ± 95% CIs.

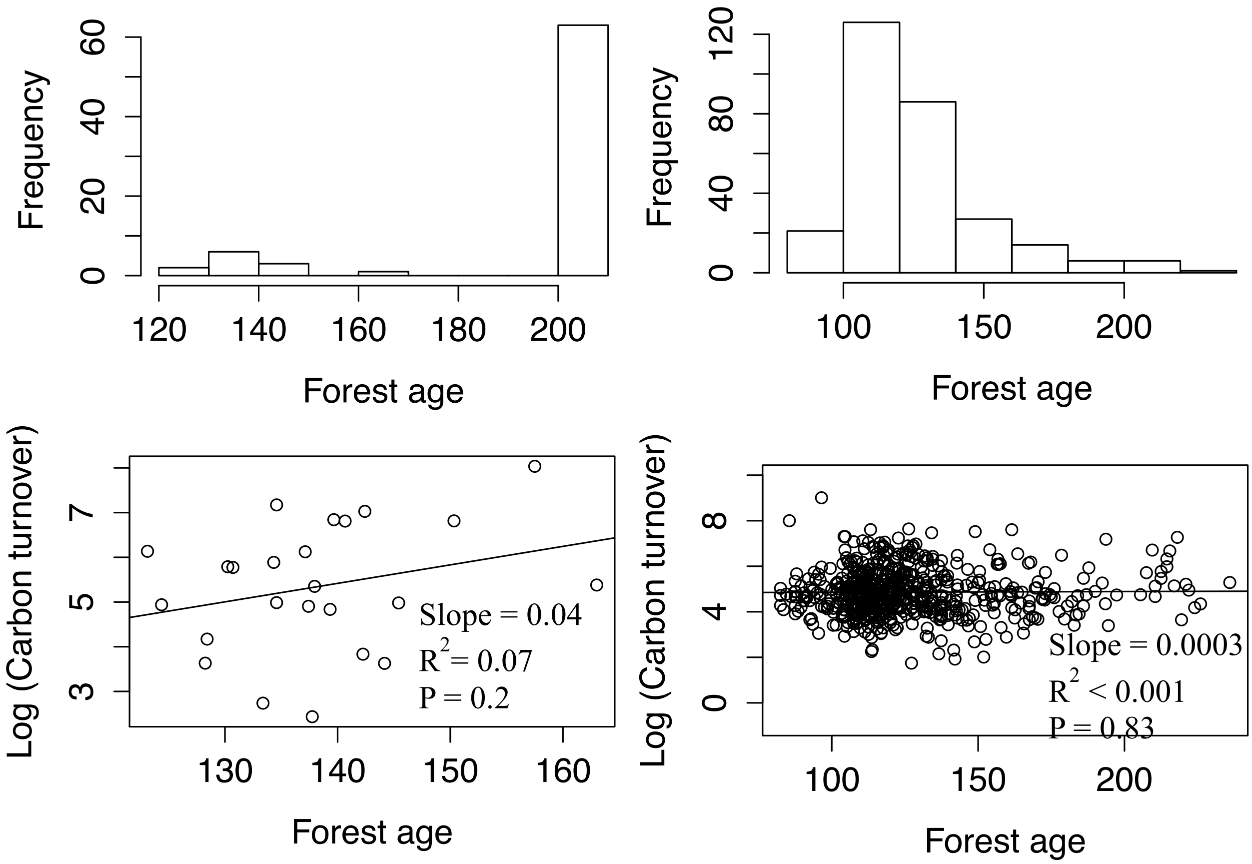

Fig. S3. (**A, B**) Frequency distribution of forest age in temperate (**A**, n = 75) and cold forests (**B**, n = 287). All forest plots derived from van Mantgem (2009) in western USA in temperate forests were more than 200 years old and were treated as 210 years old forest for purpose of plotting. (**C, D**) The relationships between aboveground living vegetation carbon turnover time and forest age in temperate (**C**) and cold (**D**) forests.

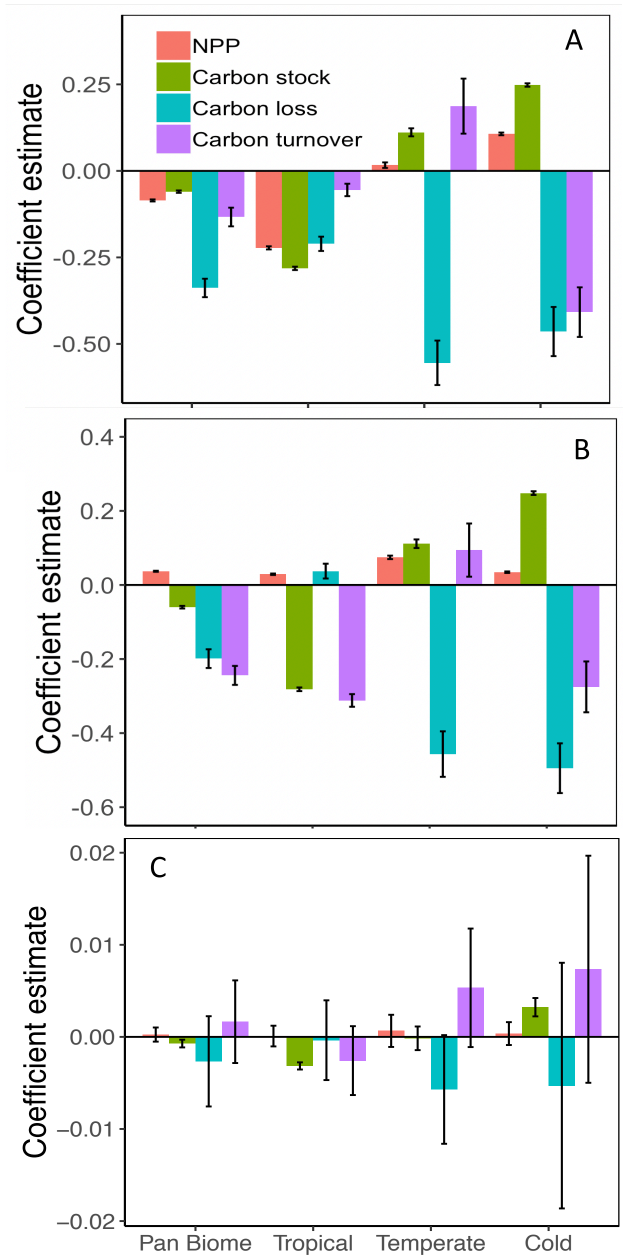

Fig. S4. (**A, B**) Temporal trend in percent change of NPP, carbon stock, carbon loss, and living vegetation carbon turnover time quantified by remote sensing data (climate NPP, A; fixed NPP, B) ranging from 1993 to 2011 across forest climate zones (0.25 × 0.25°). Temporal trend is quantified by linear mixed model accounting for each pixel in each forest climate zone as a random effect. (**C**) Temporal trend in percent change of NPP (fixed), carbon stock, carbon loss, and living vegetation carbon turnover time quantified by remote sensing data ranging from 1993 to 2011 across forest climate zones (0.25 × 0.25°) using the Friend et al (2014) method. Value of y axis is coefficient of the independent variable (time) ± 95% CIs.

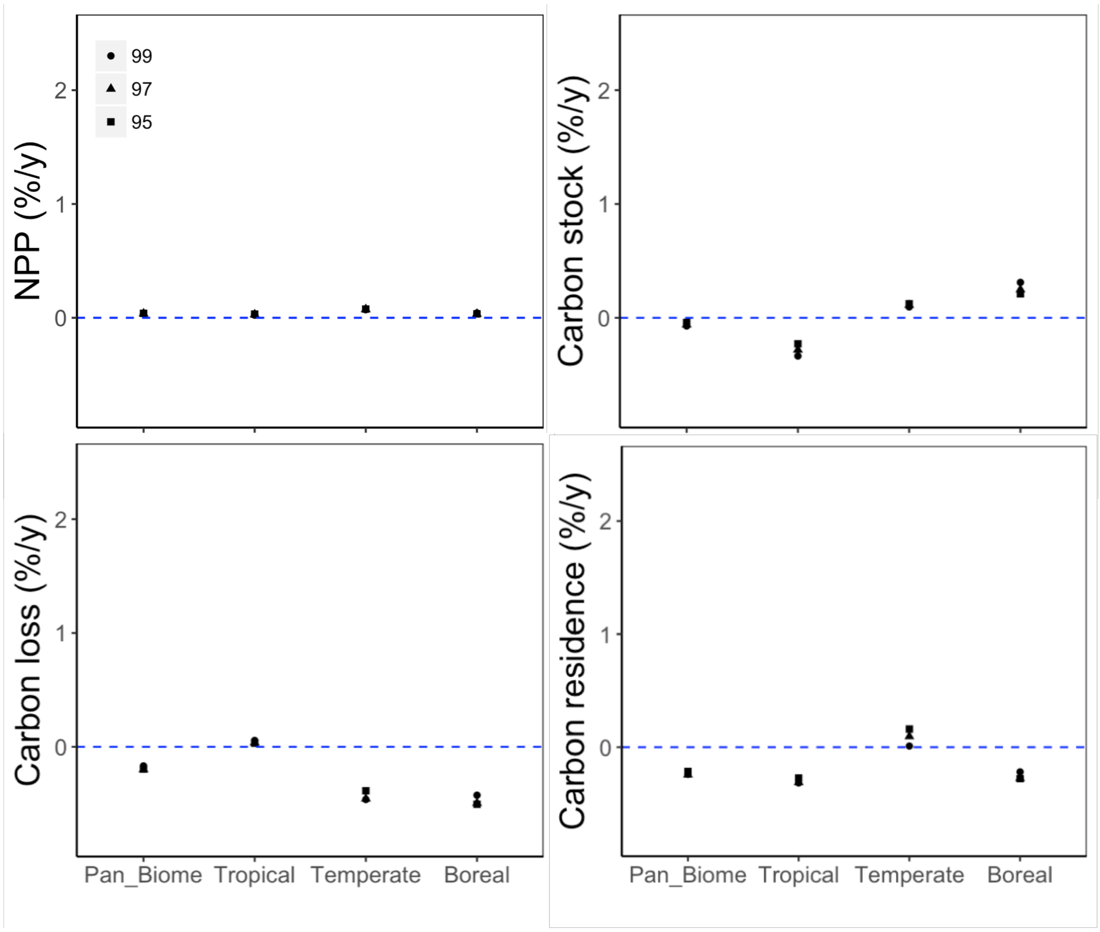

Fig. S5. Sensitivity of temporal trend of percent change in NPP, carbon stock, carbon loss, and living vegetation carbon turnover time quantified by remote sensing data to diffident standards of excluding outliers of values. “99”, “97”, “95” refer to the cases that values of percent change in NPP, carbon stock, carbon loss, and living vegetation carbon turnover time out of range of 1-99th percentile (≈2%), 3-97th percentile (≈6%) and 5-95th percentile (≈10%) are removed prior to analysis of linear mixed model.

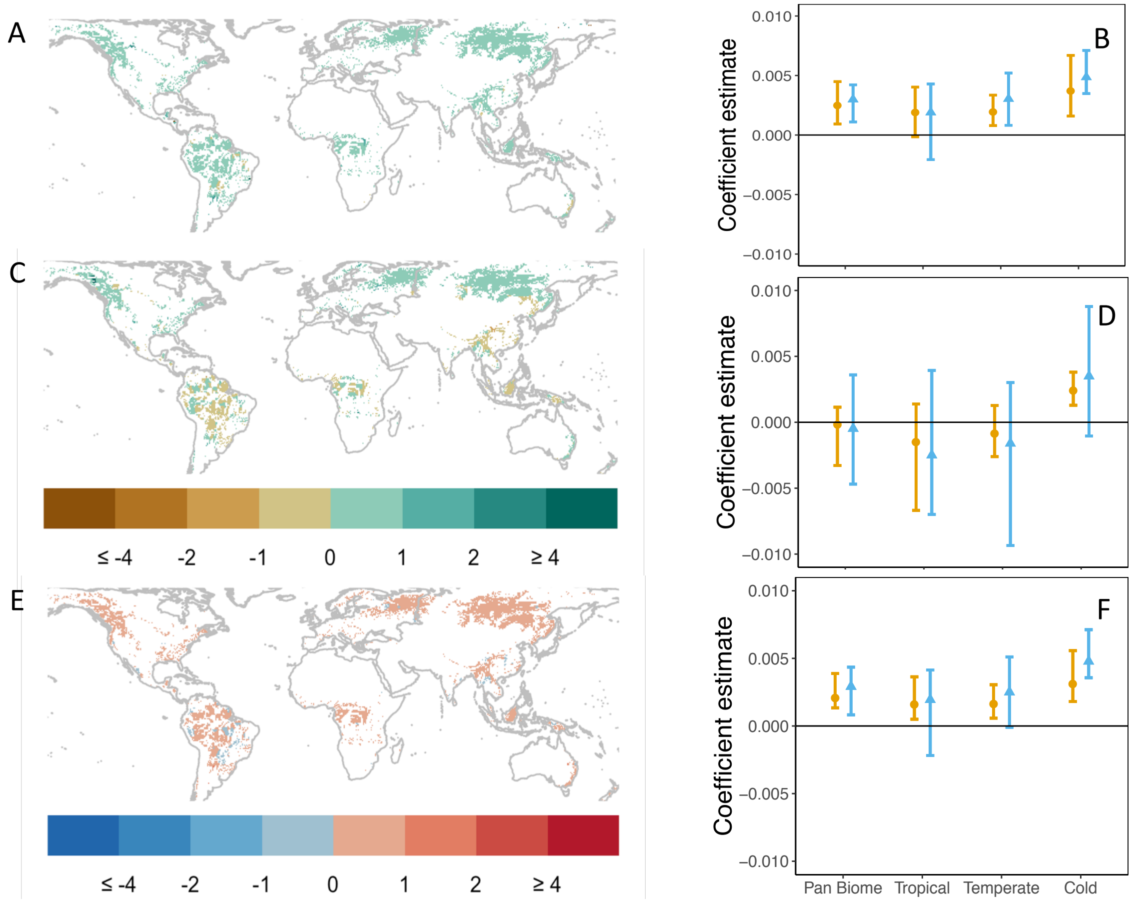

Fig. S6. Global pattern of historical (1971-2005) (**A, C, E, G**) and predictive (2006-2100) (**B, D, F, H**) temporal trend in percent change of NPP (**A, B**), carbon stock (**C, D**), carbon loss (**E, F**), and living vegetation carbon turnover time (**G, H**) quantified by eight Earth system models (CanESM2, CCSM4, GFDL-ESM2G, HadGEM2-ES, IPSL-CM5A-MR, MIROC-ESM, MPI-ESM-LR, NorESM1-M) in phase 5 of the Coupled Model Intercomparison Project (CMIP5). Temporal trend is quantified by the linear regression model and expressed as coefficient (value of y axis) of the independent variable (time) in the linear regression model.

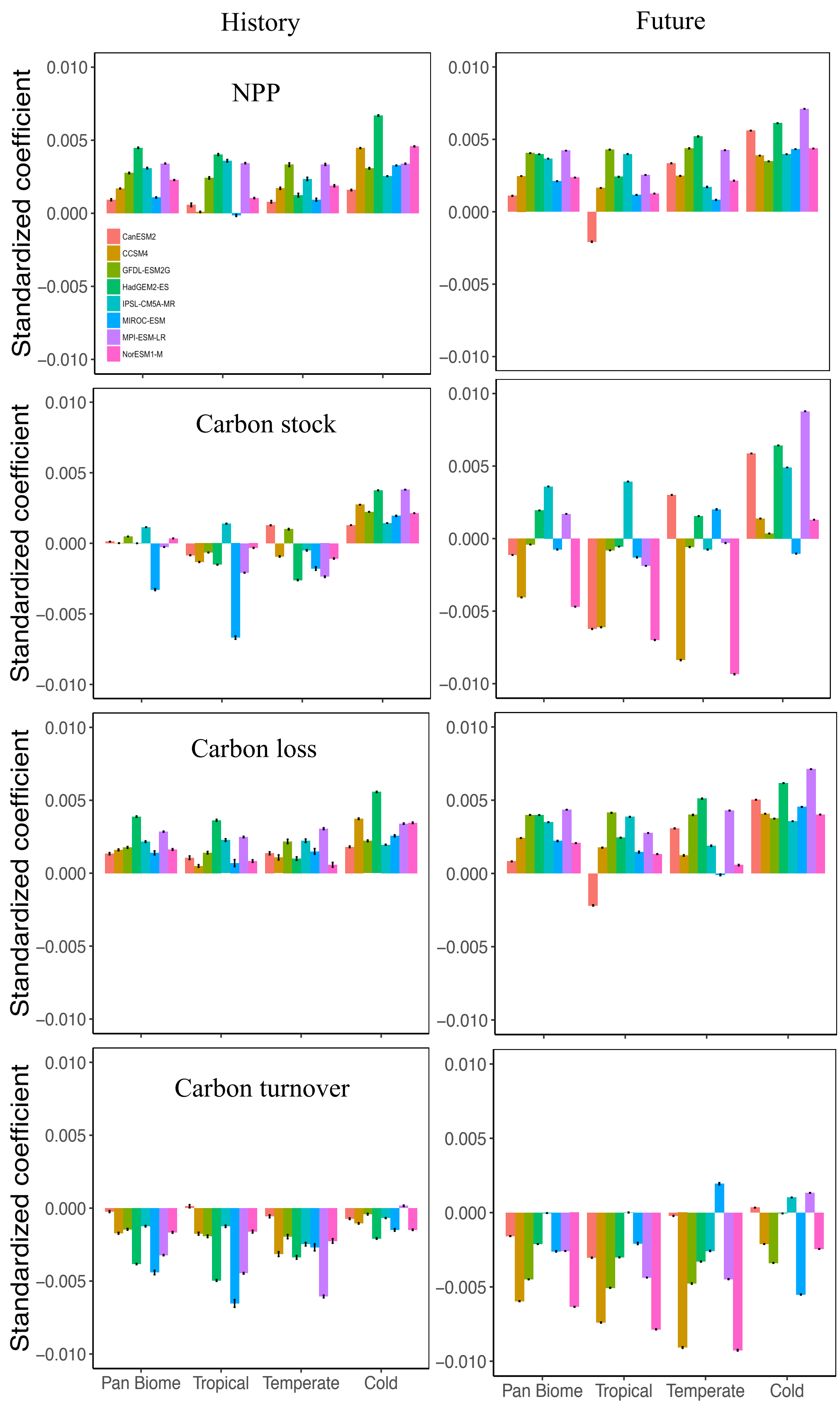
History
Future
NPP
Carbon stock
Carbon loss
Carbon turnover
Standardized coefficient
0.010
0.005
0.000
−0.005
−0.010
CanESM2
CCSM4
GFDL-ESM2G
HadGEM2-ES
IPSL-CM5A-MR
MIROC-ESM
MPI-ESM-LR
NorESM1-M
Pan Biome
Tropical
Temperate
Cold

Fig. S7. Historical (1971-2005) (**A, C, E, G**) and predictive (2006-2100) (**B, D, F, H**) temporal trend in natural log-transformed values of NPP (**A, B**), carbon stock (**C, D**), carbon loss (**E, F**), and living vegetation carbon turnover time (**G, H**) quantified by eight Earth system models (CanESM2, CCSM4, GFDL-ESM2G, HadGEM2-ES, IPSL-CM5A-MR, MIROC-ESM, MPI-ESM-LR, NorESM1-M) in CMIP5. Temporal trend is quantified by the linear mixed model accounting for each pixel in each forest climate zone as a random effect. Value of y axis is coefficient of the independent variable (time) ± 95% CIs.

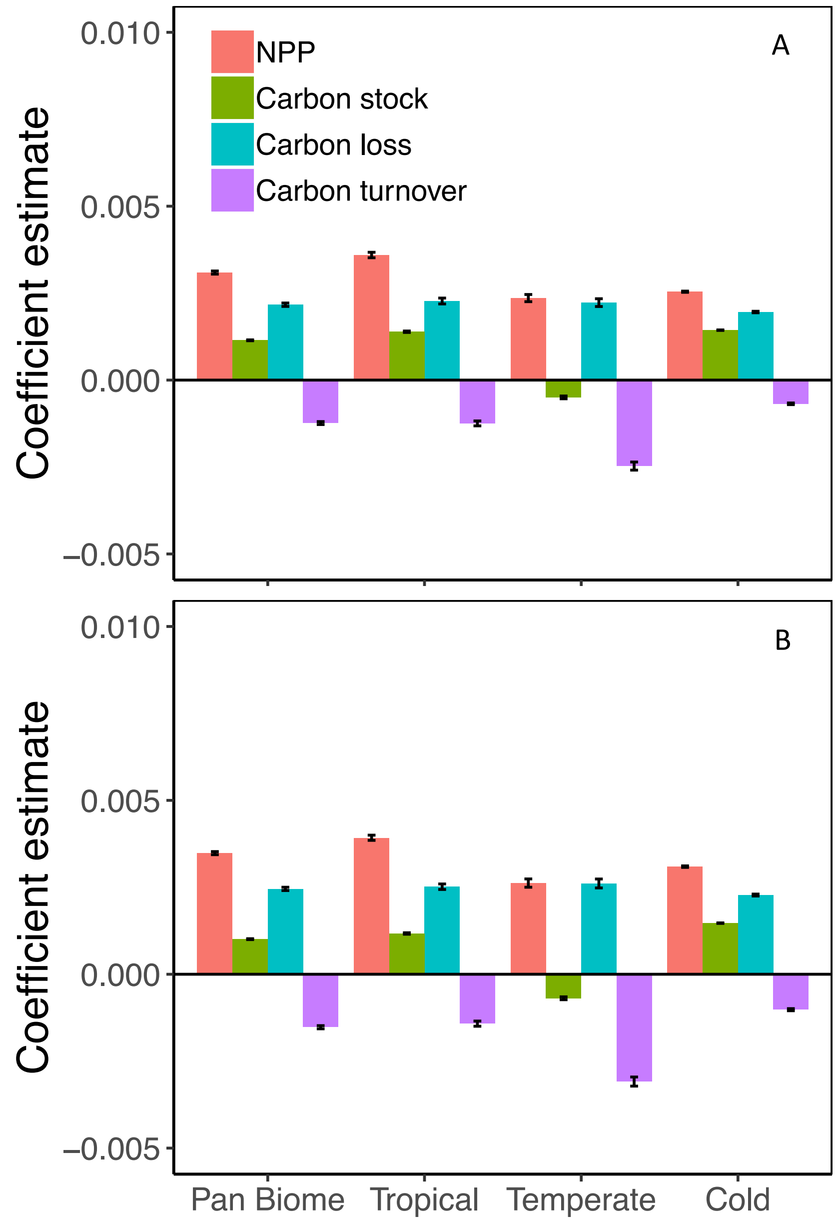

Fig. S8. Historical (1971-2005) temporal trends in natural log-transformed values of NPP, carbon stock, carbon loss from mortality, and living vegetation carbon turnover time across forest climate zones quantified from IPSL-CM5A-MR by using total NPP and vegetation carbon stock (**A**) and aboveground NPP and vegetation carbon stock (**B**).

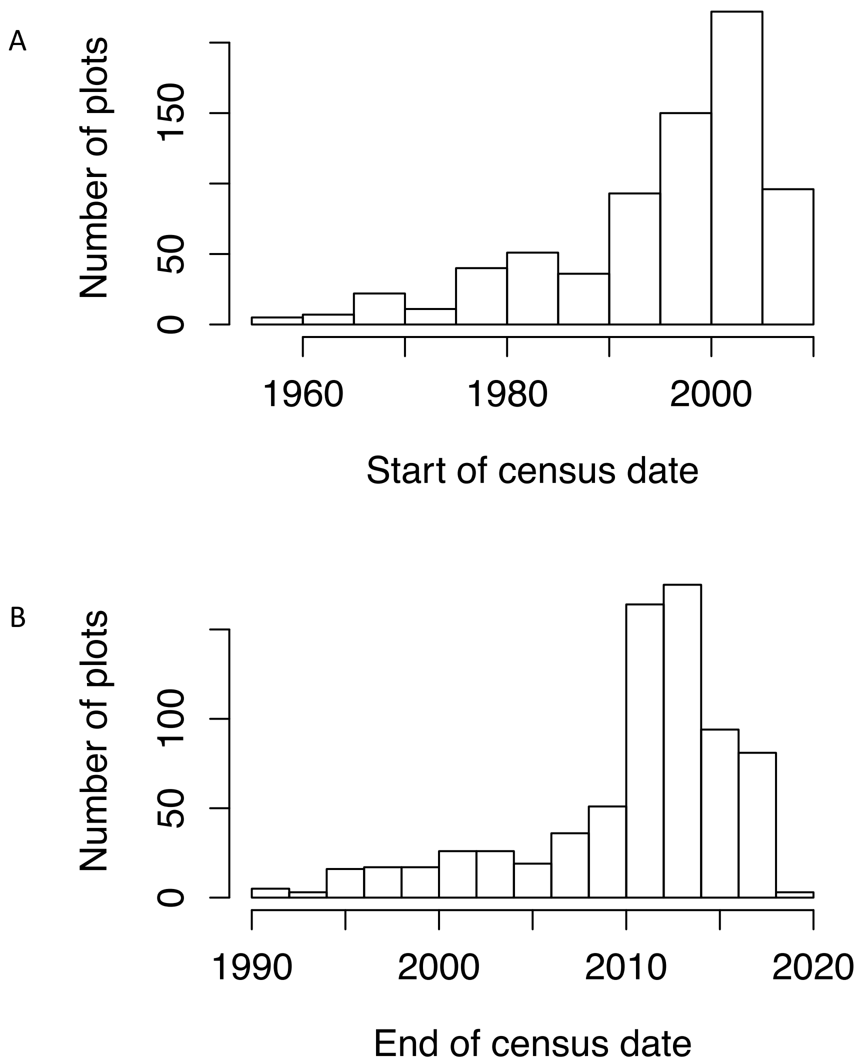

Fig. S9 Distribution of start of census date (**A**) and end of census date (**B**).

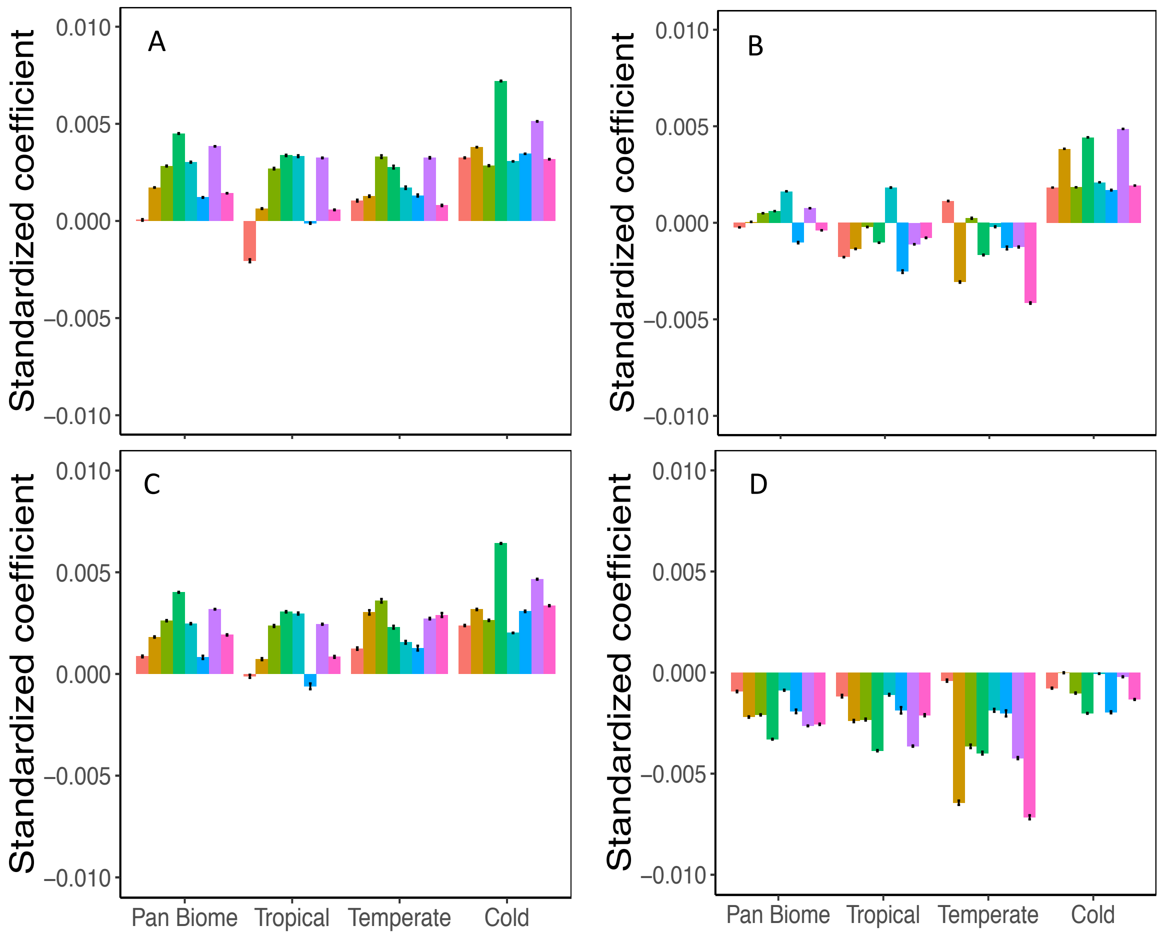

Fig. S10. Historical (1971-2018) temporal trends in natural log-transformed values of NPP (**A**), carbon stock (**B**), carbon loss from mortality (**C**), and living vegetation carbon turnover time (**D**) across forest climate zones quantified by eight Earth system models (CanESM2, CCSM4, GFDL-ESM2G, HadGEM2-ES, IPSL-CM5A-MR, MIROC-ESM, MPI-ESM-LR, NorESM1-M) in phase 5 of the Coupled Model Intercomparison Project (CMIP5). The legend is the same as Fig. S7.

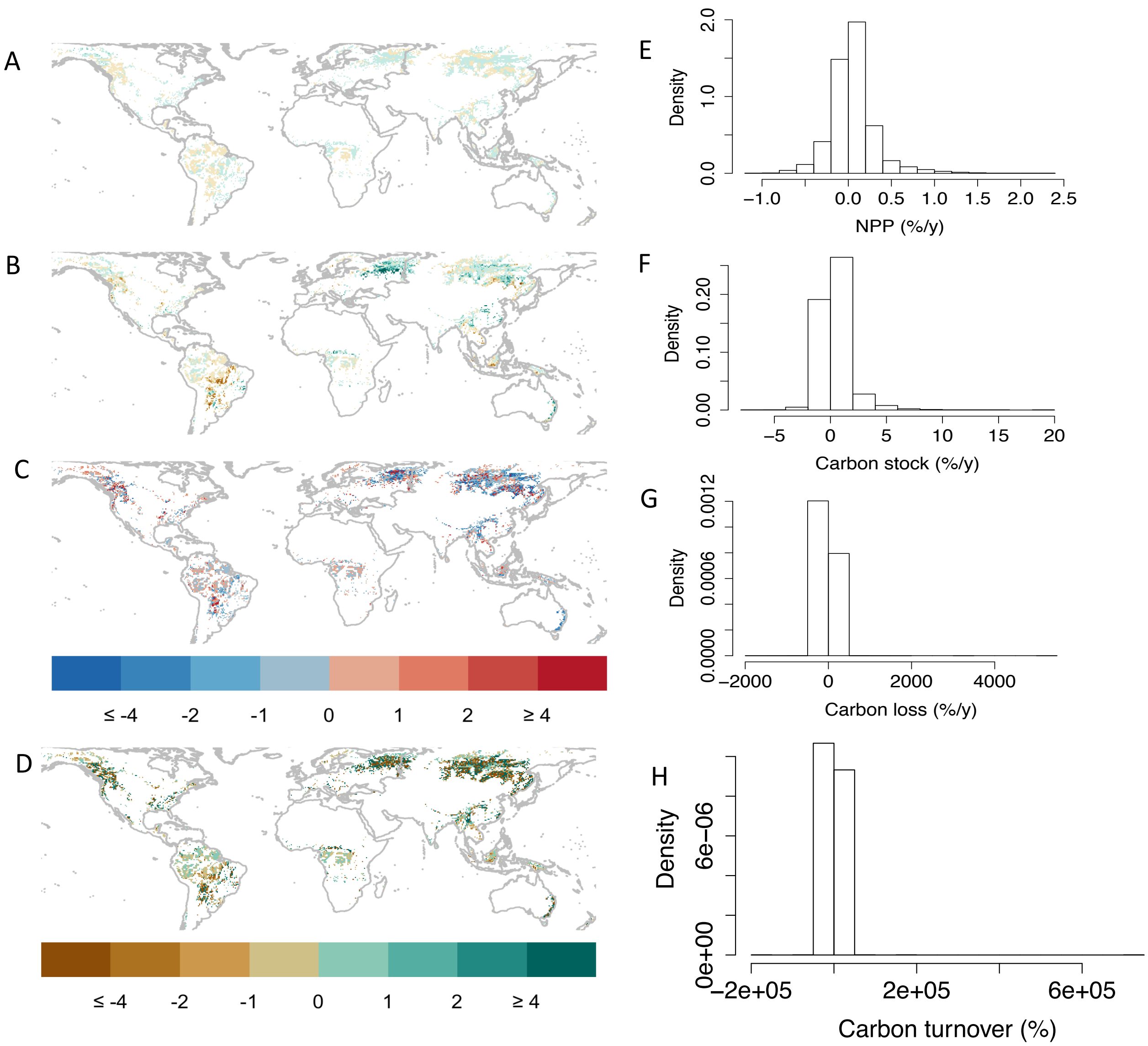

Fig. S11. (**A, B, C, D**) Global pattern of historical (1993-2011) temporal trend in percent change of NPP (**A**), carbon stock (**B**), carbon loss (**C**), and living vegetation carbon turnover time (**D**) quantified by remote sensing data. Temporal trend is quantified by linear regression models and expressed as coefficients of the independent variable (time) of the linear regression models. (**E, F, G, H**) Density distribution of temporal trend in percent change of NPP (**E**), carbon stock (**F**), carbon loss (**G**), and living vegetation carbon turnover time (**H**) in cold forests, which has the same patterns with Pan Biome forests.

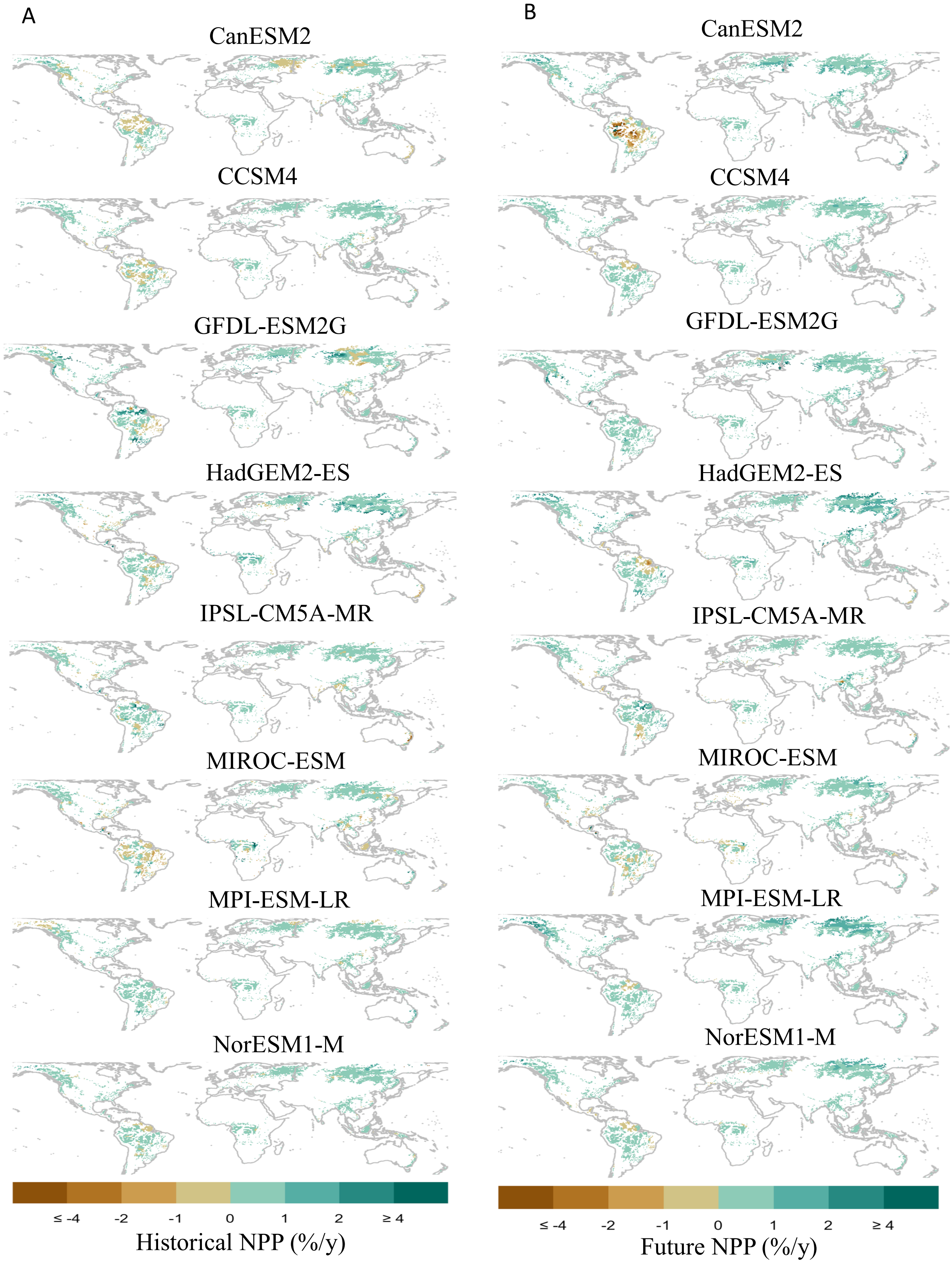
A
CanESM2
CCSM4
GFDL-ESM2G
HadGEM2-ES
IPSL-CM5A-MR
MIROC-ESM
MPI-ESM-LR
NorESM1-M
≤ -4
-2
-1
0
1
2
≥ 4
Historical NPP (%/y)
B
CanESM2
CCSM4
GFDL-ESM2G
HadGEM2-ES
IPSL-CM5A-MR
MIROC-ESM
MPI-ESM-LR
NorESM1-M
≤ -4
-2
-1
0
1
2
≥ 4
Future NPP (%/y)

956

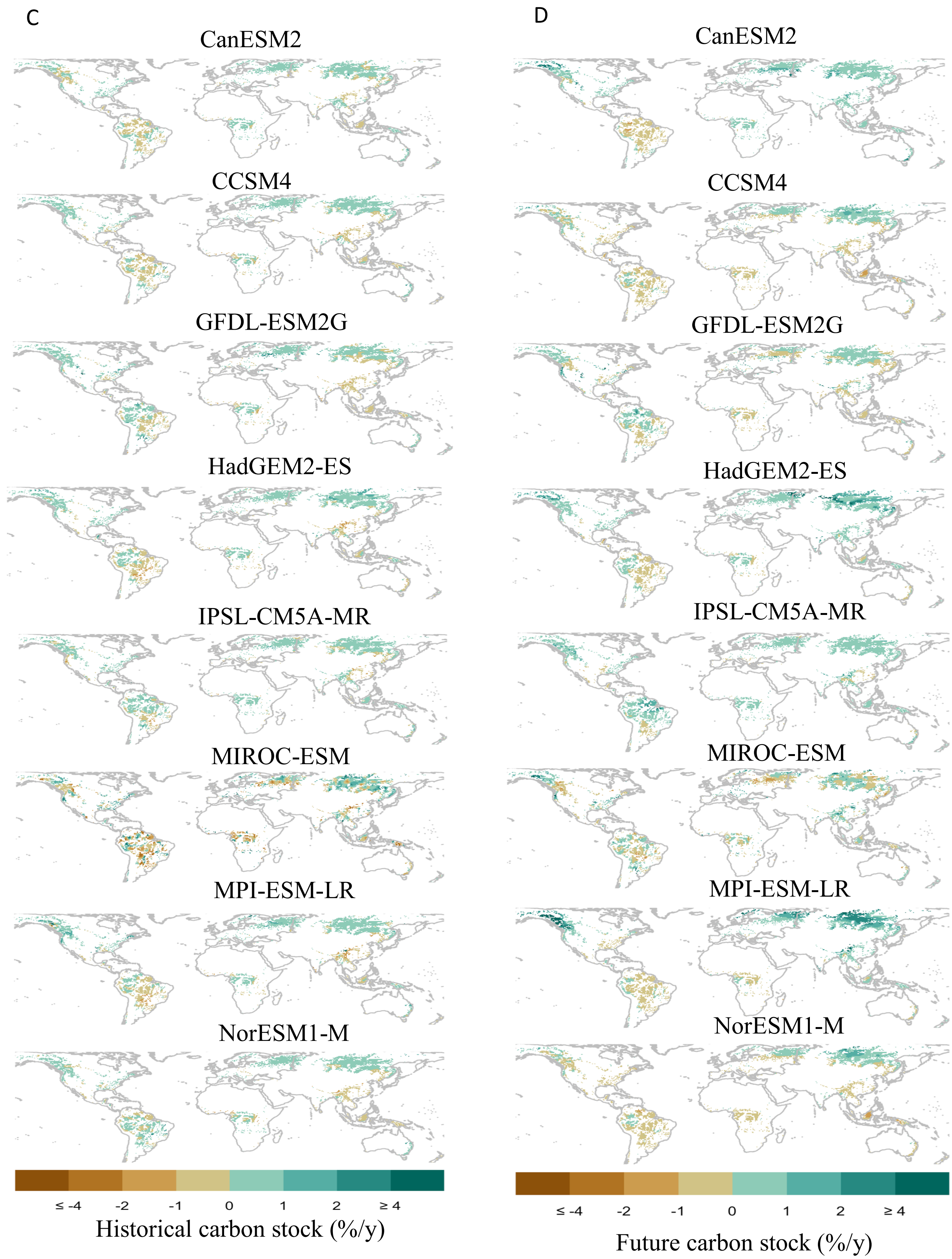

C
CanESM2
CCSM4
GFDL-ESM2G
HadGEM2-ES
IPSL-CM5A-MR
MIROC-ESM
MPI-ESM-LR
NorESM1-M
≤ -4
-2
-1
0
1
2
≥ 4
Historical carbon stock (%/y)
D
CanESM2
CCSM4
GFDL-ESM2G
HadGEM2-ES
IPSL-CM5A-MR
MIROC-ESM
MPI-ESM-LR
NorESM1-M
≤ -4
-2
-1
0
1
2
≥ 4
Future carbon stock (%/y)

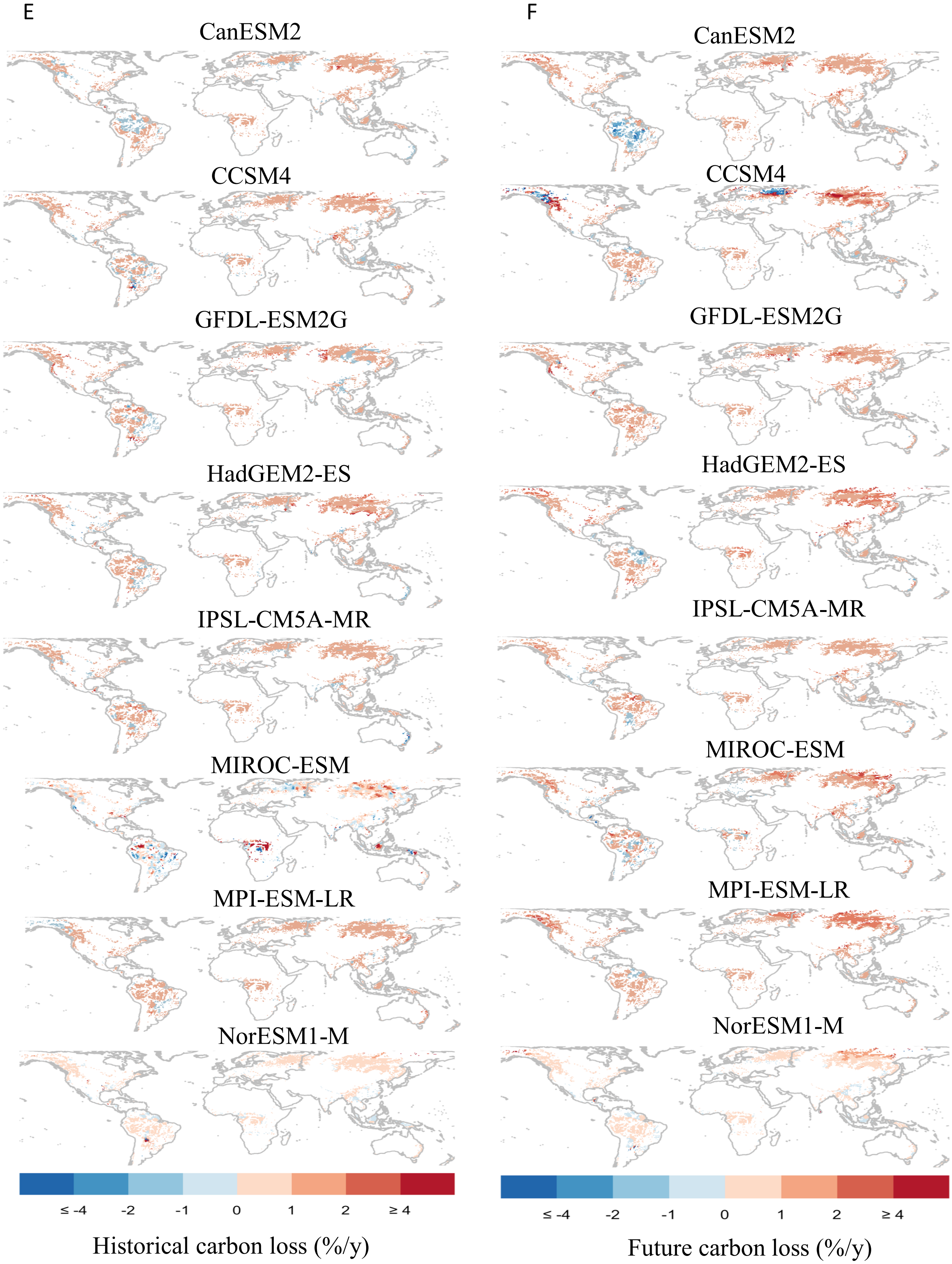
E
CanESM2
CCSM4
GFDL-ESM2G
HadGEM2-ES
IPSL-CM5A-MR
MIROC-ESM
MPI-ESM-LR
NorESM1-M
≤ -4
-2
-1
0
1
2
≥ 4
Historical carbon loss (%/y)
F
CanESM2
CCSM4
GFDL-ESM2G
HadGEM2-ES
IPSL-CM5A-MR
MIROC-ESM
MPI-ESM-LR
NorESM1-M
≤ -4
-2
-1
0
1
2
≥ 4
Future carbon loss (%/y)

958

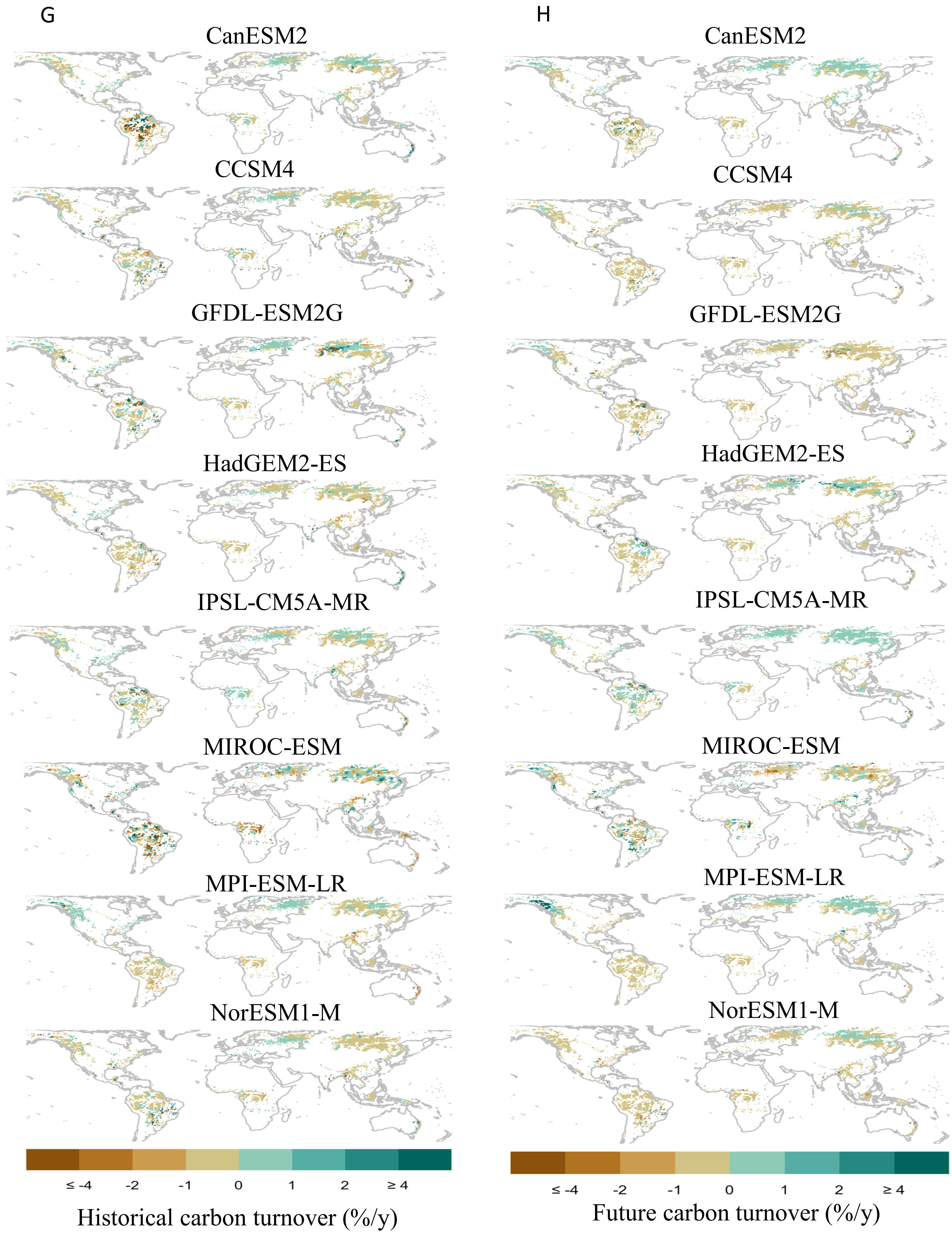
G
H
CanESM2
CCSM4
GFDL-ESM2G
HadGEM2-ES
IPSL-CM5A-MR
MIROC-ESM
MPI-ESM-LR
NorESM1-M
≤ -4
-2
-1
0
1
2
≥ 4
Historical carbon turnover (%/y)
Future carbon turnover (%/y)

Fig. S12. (**A, C, E**) Global pattern of historical (1971-2005) temporal trend in percent change of NPP (**A**), carbon stock (**C**), and carbon loss (**E**) quantified by ensemble mean of eight Earth system models in phase 5 of the Coupled Model Intercomparison Project (CMIP5). Temporal trend is quantified by the linear regression model and expressed as coefficient (value of y axis) of the independent variable (time) in the linear regression model. (**B, D, F**) Historical (1971-2005) and predictive (2006-2100) temporal trend in NPP, carbon stock, and carbon loss across forest climate zones quantified by the eight Earth system models in CMIP5. Temporal trend is quantified using the linear mixed model. Values of y axis are minimum, mean and maximum of temporal trend in eight Earth system models.

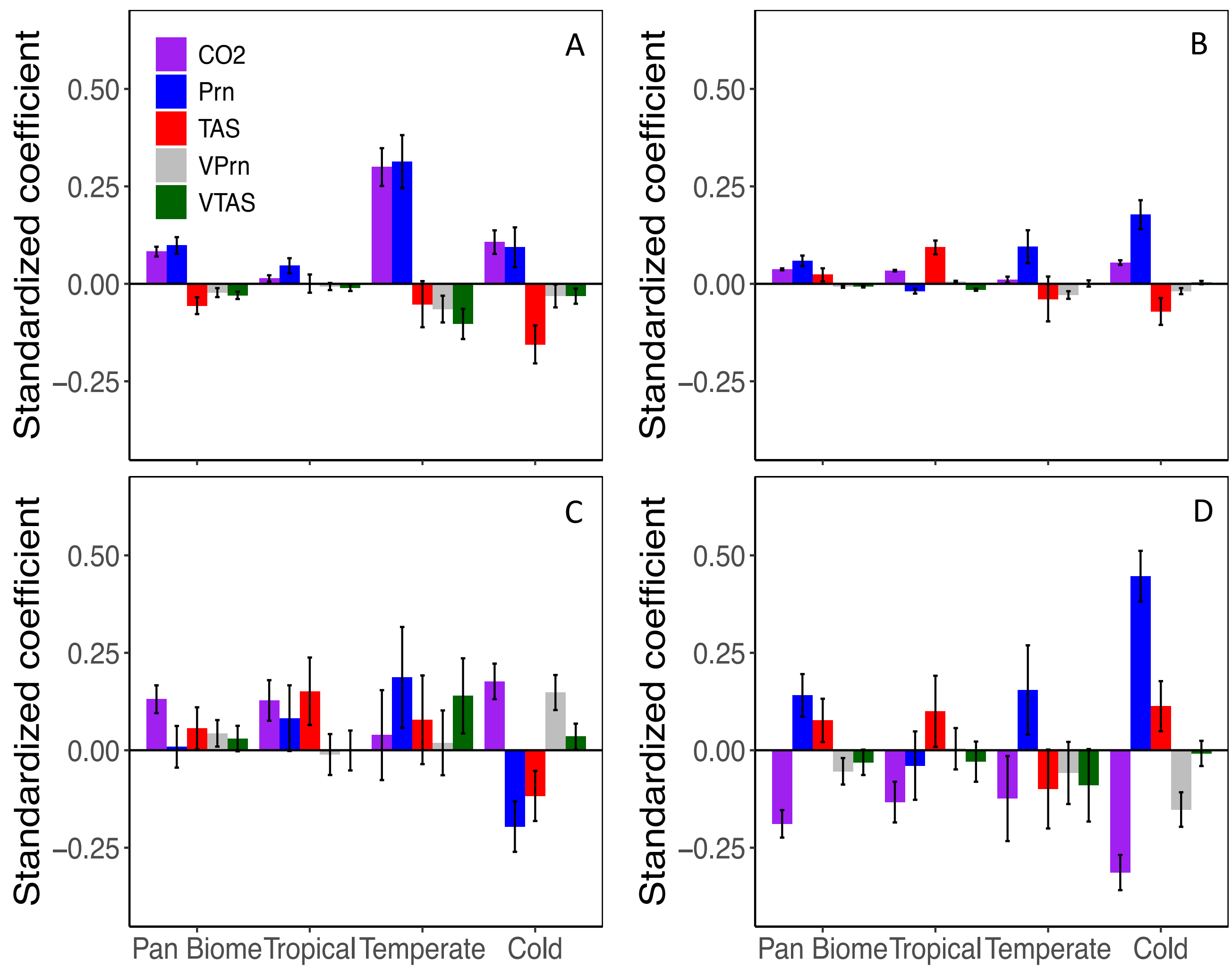

Fig. S13. Standardized response coefficients between CO_2, precipitation (Prn), temperature (TAS), precipitation anomaly (VPrn), and temperature anomaly (VTAS) and NPP (A), carbon stock (B), carbon loss (C), and vegetation carbon turnover time (D) quantified for forest plot data using linear mixed models. The data for NPP, carbon stock, carbon loss, and vegetation carbon turnover time were natural log-transformed before analysis. The y-axes are coefficients of each independent variable ± 95% CIs.

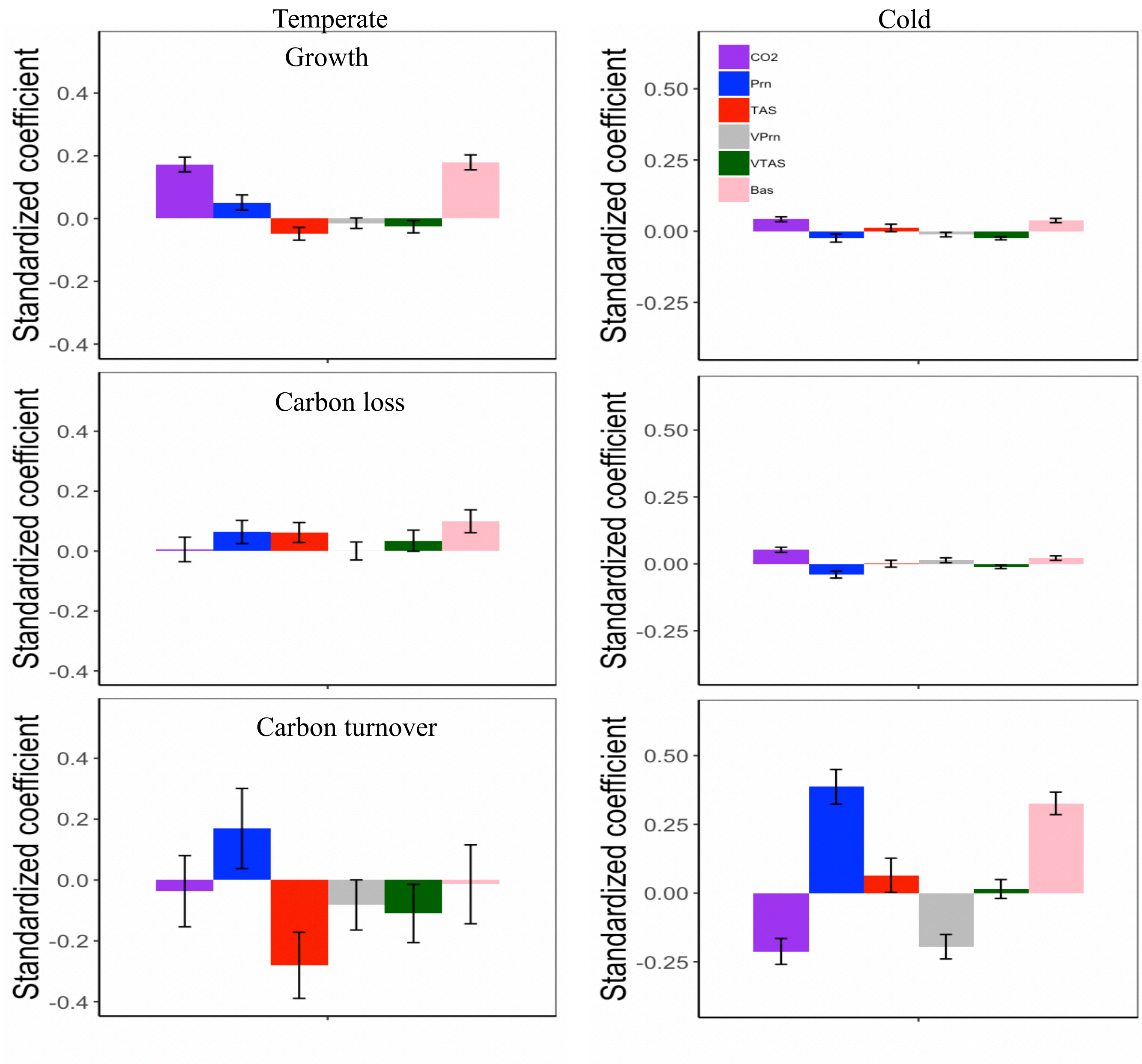

Fig. S14. Standardized response coefficients between CO_2, precipitation (Prn), temperature (TAS), precipitation anomaly (VPrn), temperature anomaly (VTem) and basal area and NPP, carbon loss, and living vegetation carbon turnover time quantified for temperate and cold forest plot data using linear mixed models. The data for NPP, carbon stock, carbon loss, and living vegetation carbon turnover time were natural log-transformed before analysis. The y-axes are coefficients of each independent variable ± 95% CIs.

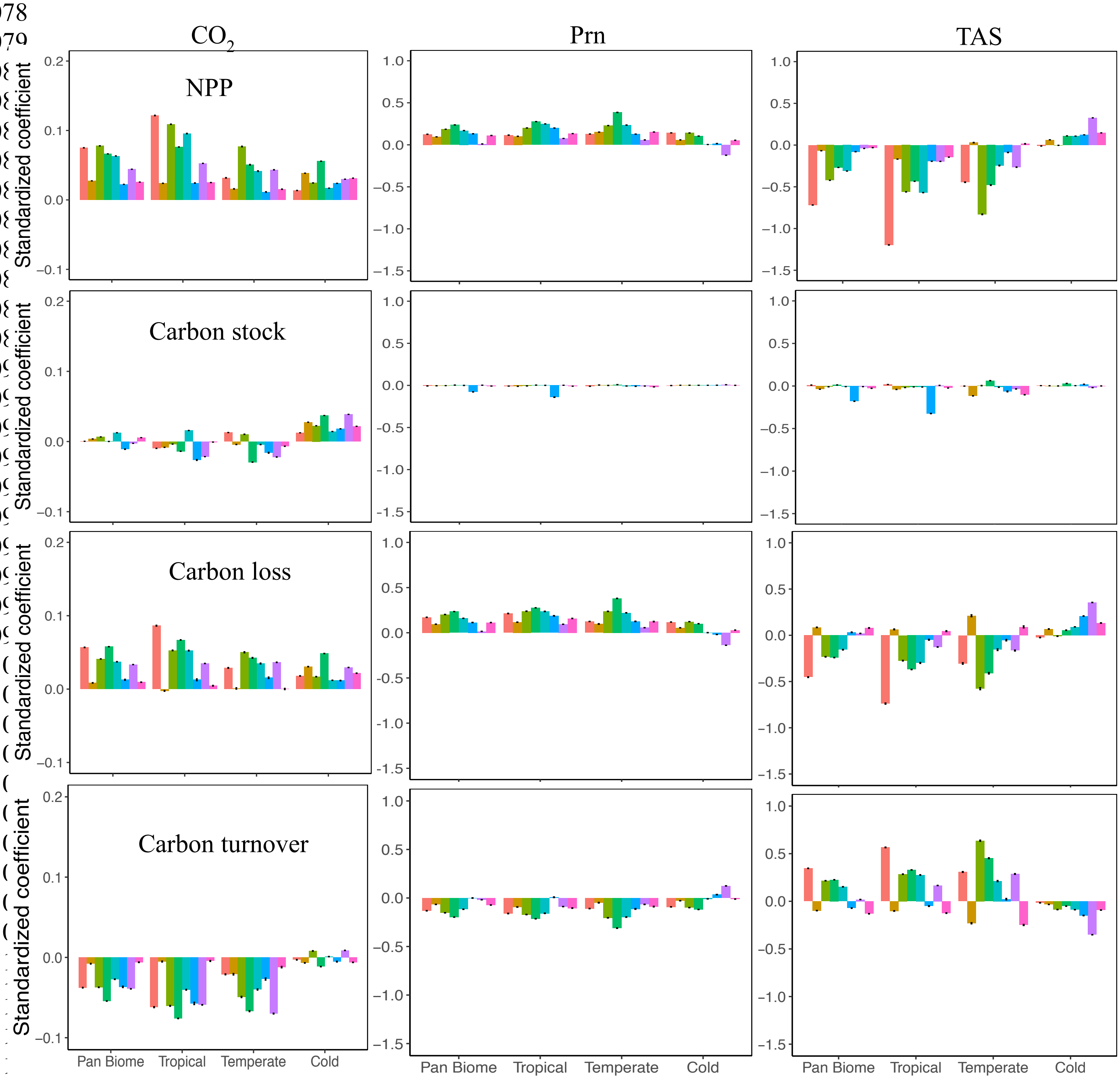

Fig. S15. Standardized response coefficients between CO_2, Prn, and TAS and natural log-transformed values of NPP, carbon stock, carbon loss, and living vegetation carbon turnover time quantified by eight Earth system models in CMIP5 and linear mixed models. Value of y axis is the coefficient of each independent variable ± 95% CIs. The legend is the same as Fig. S7.

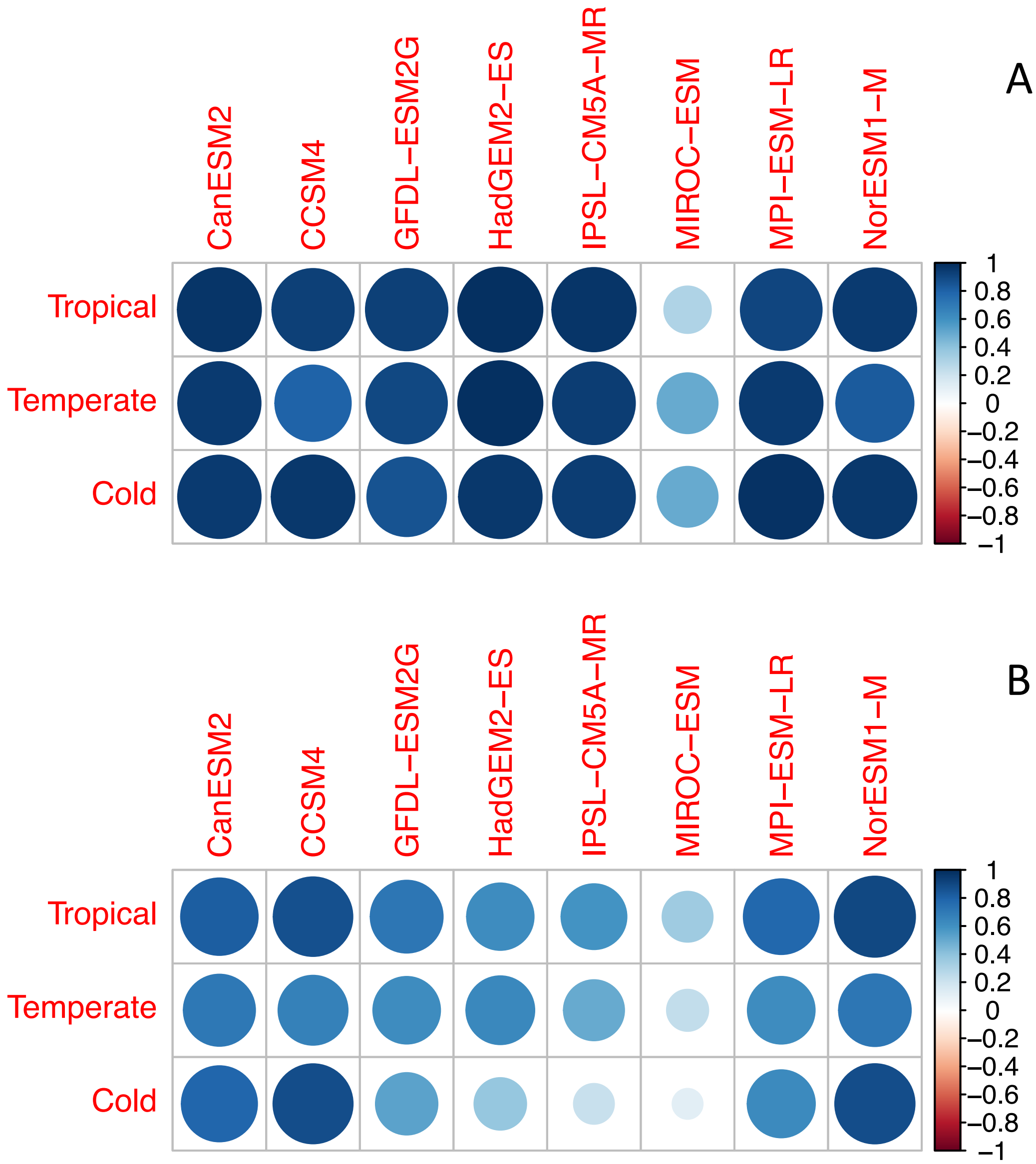

Fig. S16. Standardized response coefficients between historical (1971-2005) NPP and carbon loss (A), historical (1971-2005) carbon stock and carbon loss (B) across tropical, temperate and cold forest climate zones predicted by the eight Earth system models CMIP5. Carbon stock is quantified in the previous time step.

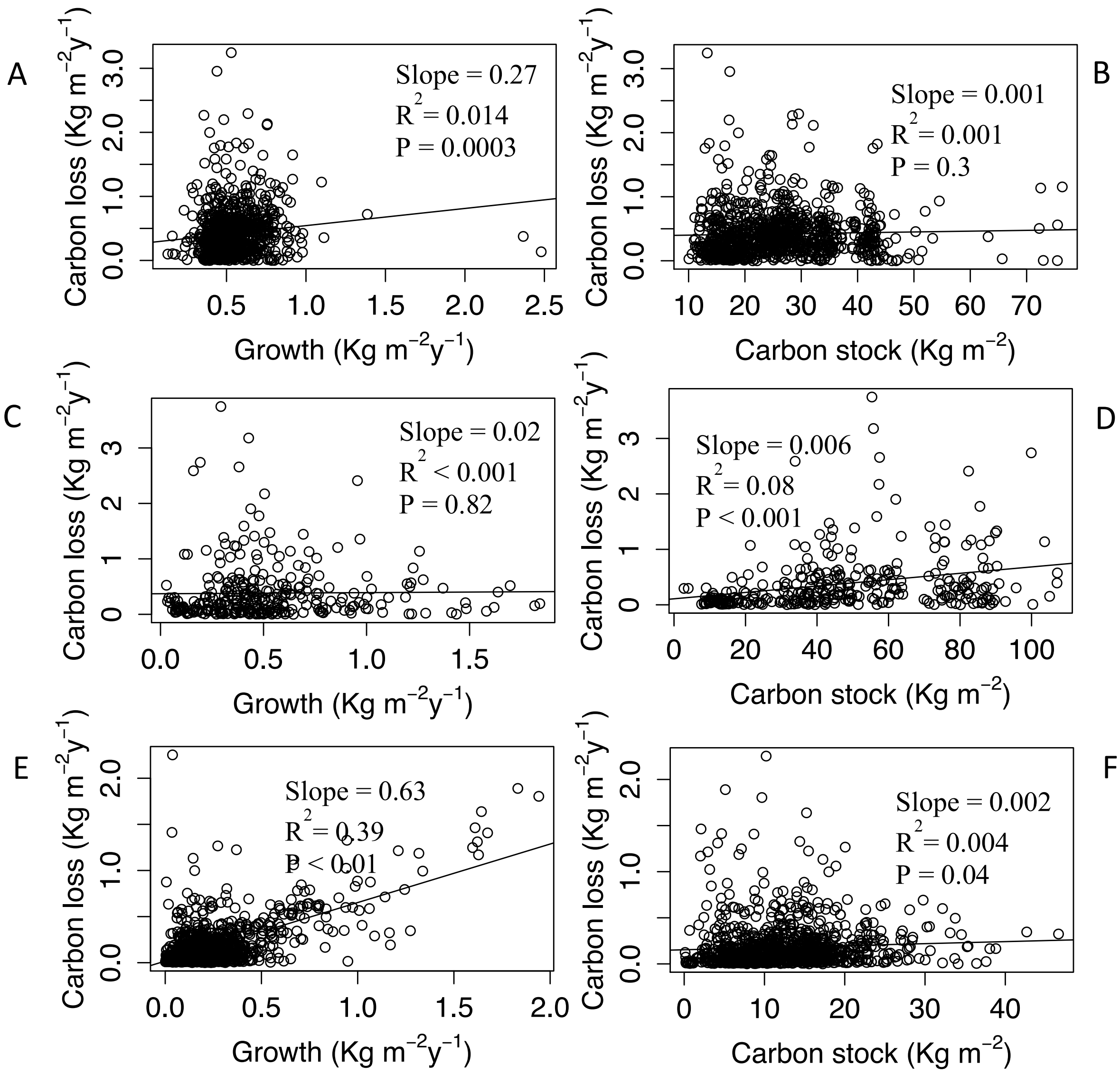

Fig. S17. The relationship between NPP and carbon loss, and carbon stock and carbon loss across tropical (A, B), temperate (C, D) and cold forest climate zones (E, F) found in forest plot data.